CCM3 AS APPLIED TO AN IDEALIZED ALL LAND ZONALLY SYMMETRIC PLANET, TERRA BLANDA 3

A Thesis

by

SALIL MAHAJAN

Submitted to the Office of Graduate Studies of
Texas A&M University
in partial fulfillment of the requirements for the degree of

MASTER OF SCIENCE

December 2004

Major Subject: Atmospheric Sciences

CCM3 AS APPLIED TO AN IDEALIZED ALL LAND ZONALLY SYMMETRIC PLANET, TERRA BLANDA 3

A Thesis

by

SALIL MAHAJAN

Submitted to Texas A&M University
in partial fulfillment of the requirements
for the degree of

MASTER OF SCIENCE

Approved as to style and content by:

Gerald. R. North
(Chair of Committee)

Kenneth P. Bowman
(Member)

Benjamin Giese
(Member)

Courtney Schumacher
(Member)

Richard E. Orville
(Head of Department)

December 2004

Major Subject: Atmospheric Sciences

ABSTRACT

CCM3 as Applied to an Idealized All Land
Zonally Symmetric Planet, Terra Blanda 3. (December 2004)
Salil Mahajan, B. Arch, Indian Institute of Technology, Kharagpur, India
Chair of Advisory Committee: Dr. Gerald R. North

Community Climate Model 3 (CCM3) is run on an idealized all land zonally symmetric planet (Terra Blanda) with no seasonality, no snow and fixed soil moisture to obtain a stationary time series effectively much longer than conventional runs with geography and seasons. The surface temperature field generated is studied to analyze the spatial and temporal spectra, estimate the length scale and time scale of the model, and test the linearity of response to periodic and steady heat source forcings. The length scale of the model is found to be in the range of 1000-2000 km and the time scale is estimated to be 24 days for the global average surface temperature field. The response of the global average temperature is found to be fairly linear to periodic and the steady heat source forcings. The results obtained are compared with the results of a similar study that used CCM0. Fluctuation Dissipation theorem is also tested for applicability on CCM3. The response of the surface temperature field to a step function forcing is demonstrated to be very similar to the decay of naturally occurring anomalies, and the auto-correlation function. Return period of surface temperature anomalies is also studied. It is observed that the length of the data obtained from CCM3, though sufficient for analysis of first and second moments, is significantly deficient for return period analysis. An AR1 process is simulated to model the global averaged surface temperature of Terra Blanda 3 to assess the sampling error associated with short runs.

To my family, for always being there for me.

ACKNOWLEDGMENTS

This work would not have been possible without the help of some people. I am forever, indebted to Dr. G. R. North for giving me an opportunity to be a part of the Department of Atmospheric Sciences. He has been the chair of my graduate committee, constantly providing guidance and encouragement. I would also like to thank Dr. K.P. Bowman for his guidance and critique and answering all my questions. I woud also like to thank my other graduate committee members, Dr. Benjamin Giese and Dr. Courtney Schumacher for their encouragement, support, and inputs on my thesis. I am grateful to Dr. R. Hetland for agreeing to substitute for Dr. Giese on the final exam, and reviewing and critiquing my work. Thanks are also due to Dr. R. Saravanan who read and commented on my thesis.

I would like to sincerely thank Mr. Harold J. Haynes for his support through the Haynes Endowed Chair in Geosciences.

Dr. Craig J. Collier and Dr. Tatiana Erukhimova have helped me a great deal in setting up CCM on my account on K2, and I take this opportunity to thank them. With their help, I have been able to save a tremendous amount of time which might have been required to set up CCM, had it all been to myself. I would also like to thank Stephanie Tice who has helped me a lot with IDL programming. Last, but not the least, thanks are due to Qiaoyan Wu for helping me with every little thing.

TABLE OF CONTENTS

LIST OF FIGURES

FIGURE Page

FIGURE Page

FIGURE Page

CHAPTER I

INTRODUCTION

The composition of the earth system with land, mountains, oceans, snow, ice, etc. is such, that there are various time scales associated with the climate variables. The time scales of the atmosphere range from days to years (Leung and North, 1991). These varied time scales result in varied response times to fluctuations within the system, making it difficult to identify a signal. The total variation of a field can be considered as a sum of externally forced (which is usually the signal) and natural variability. External variability is caused by changes in external forcing, for example changes in solar radiation or changes in ocean can cause a variability in the atmosphere (Leung, et al., 1991). Natural variability is associated with the dynamics of the atmosphere, and usually has shorter time scales than those of external variability.

To identify the variability associated with external forcing, it is necessary to understand the natural variability, and then filter it out from the total variability. Natural variability is considered as noise in various studies (Chervin, 1986; Hasselmann, 1979). To understand the natural variability, the statistics of this noise needs to be studied. However, real data records are usually not long enough to make statistically precise assessments and characterizations of the natural variability. The best way to generate data is to use numerical climate models, as they provide the versatility to run controlled experiments with the possibility of varying the sundry parameters associated with the climate system. Climate models that replicate the earth system however suffer from the disadvantage of consuming a lot of computer time. Even with computer models it is expensive to generate enough data required

---

The journal model is *Journal of Climate*.

for the analyses of the Earth system. In this study, enough data has been generated to study the land-atmosphere noise statistics, by removal of other components and complications of the Earth system from the model. The model used here is a modification of a General Circulation Model (GCM), developed by National Center for Atmospheric Research (NCAR), called the Community Climate Model 3 (CCM3). The modified earth system of the model is termed Terra Blanda 3. It is an emulation of a planet generated by Leung and North (1991), Terra Blanda, but this time using a newer implementation of the CCM.

Once the natural variability of the system is elaborated, the response of the system to external forcings and its sensitivity can be studied. The modeled system can now be perturbed in various manners to study its response, and thus aid in estimating the response of the real system. There have been arguments about the linearity of response of the earth system. Stone (1978) argued about the non-linearity of response of the diffusion process. Lorenz (1979) showed that some of the responses of the 500 mb height field of the real earth system to large scale forcings were linear. North et al. (1992) showed that the response of the surface temperature field on Terra Blanda to large-scale forcings was fairly linear. In this study external forcings are applied to Terra Blanda 3 using CCM3 to test the linearity of response and compare the sensitivity of CCM3 to these external forcings to its natural variability.

The presence of extremes in the natural variability of a system is also studied. By definition, the occurrence of extremes in natural variability is rare, and to generate enough data using the models requires a lot of computer time. Thus, the field whose response is being studied needs to be modeled by a simpler model. The simplified model can be used for studying the extremes of a field. In this study, a simpler model is created to fit the surface temperature field data on Terra Blanda 3 generated by CCM3.

The simulation of the Earth system, and using the simulation to analyze the real Earth is not assumed to provide precise insight into the climate, however close approximations can be made out of these simulations that are true to the real world with a certain confidence level.

CHAPTER II

PREVIOUS STUDIES

Leung and North (1991) studied the noise statistics of the surface temperature field associated with natural variability of a specific GCM simulation, CCM0 as applied on Terra Blanda. Huang et al. (1991) also performed several experiments with Terra Blanda, and showed that its circulation statistics are plausible. North et al. (1992) also performed experiments with CCM0 as applied to Terra Blanda. Terra Blanda was an all land planet with no topography. The model ran at perpetual equinox and had other characteristics as described below in the GCM simulation section, yielding a stationary time series. They noted that these idealizations effectively lengthen the time series generated by a factor of 1000, over the conventional runs, which incorporate geography and seasons. In their study, they showed that the response of the surface temperature field of Terra Blanda to small but interesting forcings is linear, when the non-linearity associated with the snow-albedo feedback mechanism is removed. They studied the surface temperature field of Terra Blanda, and found that the variance of the zonal average temperature increases sharply from the mid latitudes to the poles.

Leung and North (1991) found that the correlation length of the zonal averaged temperature over different latitudes was almost constant, about 1200 km, and was a little longer at the tropics. In a subsequent paper, they estimated that the length scale of the surface temperature field in the model is between 1000-2000km on the globe, in agreement with the length scale evaluated from real data from stations around the world (Hansen and Lebedeff, 1987). Leung and North (1991) also studied the variance distribution of the spatial spectrum using the spherical harmonic basis functions, and found that the variance is not equally distributed between the zonal wave numbers

for a spherical harmonic degree suggesting spherical in-homogeneity of the surface temperature field. They also found that the grouped variance of zonal wave-numbers for a spherical harmonic degree is the maximum at degree 8 or 9 and increases linearly up to spherical harmonic degree 8 or 9, and then reduces, but breaks in slope at degree 15 because of the rhomboidal truncation at degree 15 used in CCM0. The linearity up to degree 8 was explained by the spatial homogeneity of the surface temperature field up to degree 8 implying a white spectrum of the variance distribution or equal variance among zonal wave numbers up to degree 8.

Leung and North (1991) also showed that the maximum variance in the temporal spectrum was explained by planetary waves with periods ranging from 10 to 60 days, and suggested that a change in the variance structure can serve as a signal for external forcing. In the subsequent paper, North et al. (1992) probed the spectrum of the spherical harmonic coefficients of the surface temperature field for change in the spectrum to detect signals of a sinusoidal forcing of the sun on Terra Blanda. This study analyzes the data from a more sophisticated atmospheric model, CCM3. The length scale will be evaluated and compared to that obtained by CCM0 version of Terra Blanda. The variance distribution across the spectrum is analyzed and checked for any breaks in the variance distribution plot, as CCM3 uses a triangular truncation instead of the rhomboidal truncation used in CCM0, and no breaks are expected.

North and Cahalan (1981) and Leung and North (1991) found that for the EBMs that were forced with noise processes each of the spherical harmonic modes exhibited behavior that was very similar to first order auto-regressive (AR1) processes. In a subsequent paper, North et al. (1992) showed that the global average temperature for Terra Blanda is also well represented by a first order auto-regressive (AR1) process with an auto-correlation time of 30 days. Also, the higher modes of the spectral transform from Terra Blanda are well represented by AR1 processes. In this study, a

first order auto regressive process is used to model the global average temperature and other spherical harmonic modes obtained from Terra Blanda 3 and the time-scales of the two models compared.

North et al. (1992) forced the model with periodic sinusoidal variations of the solar constant, and showed that the response of the global average temperature and higher modes to such large spatial scale forcings was linear with very little power diverted into higher harmonics. They forced a 20% periodic variation of the solar parameter with a period of 30 days. They found that the periodic response in the 30 days time period in the spherical harmonic coefficients T_{00}, T_{20}, and T_{40} was statistically significant, with the absence of peaks at higher harmonics of the 30 days period, implying that the response to such forcings was linear. When they further raised the amplitude to 40%, peaks were observed at frequencies corresponding to time periods of 15 and 10 days, but the variance in these harmonics was evaluated to be less than 1% compared to the variance in 30 days period. They performed similar experiments with amplitudes of the forcing of 10% and 5%, and found that the response of the surface temperature field to the solar forcing was a linear function of the amplitude of the forcing. A similar experiment is done using Terra Blanda 3 to check its linearity of response to external forcing at large scales.

North et al. (1992) also applied a zonal forcing to Terra Blanda by placing a steady and finite latitudinal ring heat source at the mid-latitudes and studied its response on the surface temperature field. They found that the response of the surface temperature field had unphysical anomalous peaks at the poles, and showed that the spurious behavior of the model was due to the truncation at degree 15, and validated their proposal by running a similar simulation with an energy balance model (EBM) which uses the Green's function (North and Cahalan, 1981) to evaluate the surface temperature field owing to diffusion, truncated at degree 15 and degree

30. The EBM truncated at degree 15 showed a similar response, while the degree 30 truncated model behaved reasonably. A similar experiment is conducted in this study with Terra Blanda 3 to verify their analysis, and check for the linearity of response of the surface temperature field at the center of the site of the forcing.

Leith (1975) proposed that the Fluctuation Dissipation Theorem (FDT) could be applied approximately to the climate system for large-scale studies. FDT states that in certain systems with natural internal fluctuations, the climate sensitivity to an externally imposed time dependent perturbation can be related to the natural variability statistics of the undisturbed system (North et al., 1993). North et al. (1993) checked the FDT as applied to the surface temperature data obtained from Terra Blanda, and found that it held reasonably well, if the temperature field was considered to be uncoupled to the other components of the model. They applied a step function solar forcing and compared the adjustment time of the model to the auto-correlation time of the model. Also, the decay of naturally occurring surface temperature anomalies was compared to the auto-correlation function. They proposed that a reasonable relationship between the adjustment time and the autocorrelation time is a good test for the sensitivity of a model. In this study, such a test is conducted on Terra Blanda 3 to test the sensitivity of CCM3.

Recurrence times of anomalies and detection of trends in extreme values are of interest in climatology. Zhang et al. (2004) studied the extreme value distribution of precipitation from data obtained from a site. The distribution of the maxima of a sample of identically distributed variables converges to a generalized extreme value distribution. The return period of extremes can be evaluated from these functions (Coles, 2001). Zhang et al. (2004) simulated an exponential function that fit the precipitation data, and obtained an extreme value distribution function. In this study, surface temperature field data obtained from Terra Blanda 3 will be modeled

to find such a trend in its extreme value distribution. The study of extremes in data obtained from climate models is generally used for return period analysis with return periods of 100 days or less (Frei, 2003). The data available from models, as well as real data, are not enough for precise statistical estimates for periods greater than the 100 days and are prone to errors if used for extrapolation for return periods much greater than 100 days (Frei, 2003). Recent studies (Kharin and Zweirs, 2000) have used the extreme value statistics for analysis of extremes with greater return periods, and have been demonstrated to have considerable sampling error. The sampling error associated with extremes is illustrated for the global average surface temperature in this study.

CHAPTER III

GENERAL CIRCULATION MODELS (GCM'S)

A. CCM0 and CCM3

There has been a significant change in the Community Climate Model developed by NCAR, since the introduction of CCM0, to its latest version CAM 3.0. CCM0 was a very simplistic delineation of the earth's atmosphere. It was a spectral model with rhomboidal truncation of degree 15 with a latitude-longitude grid resolution of 4.5° x 7.5°. It had nine-layered finite-difference vertical scheme. It used simple convective schemes, and incorporated convective adjustments, stable condensation, vertical diffusion, and surface energy balance. It also included include cloud and snow feedbacks and a very simple soil moisture scheme (Acker et al., 1996). CCM3 is a version prior to CAM 3.0. It has a triangular resolution of spherical harmonic degree forty-two (T42). The spatial latitude-longitude grid resolution of CCM3 is 2.8° x 2.8°, with significantly improved radiation schemes, diffusion processes, hydrological cycle, and surface energy exchanges. It has an 18-layered vertical finite-difference scheme. CCM3 is an optimized code with multitasking capabilities, and a much more flexible memory management scheme (Acker et al., 1996).

CCM3 is a spectral climate model with a T42 horizontal resolution, and 18 vertical levels with a lid at 2.917 mb. The time integration method used in CCM3 is semi-implicit. It treats the dry dynamics by the spectral transform method and uses a biharmonic horizontal diffusion operator. It uses a terrain following vertical coordinate. (Kiehl et al., 1996) For controlling the transportaion of various scalar fields like advection of water vapor, chemical constituents, it uses a shape preserving semi-Lagrangian transport scheme (Williamson and Rasch, 1994). The radiative transfer

in the model is represented by clear and cloudy atmospheric columns separately. Solar absorption is calculated by the Delta-Eddington approximation (Briegleb, 1992). It incorporates trace gases in the longwave parameterization and in the shortwave parameterization it incorporates background aerosols with optical depth of 0.14. CCM3 incorporates radiative properties of ice-clouds and diagnostics of convective and layered cloud amount. The model is in agreement with real observations of cloud forcings. Also, the globally averaged clear sky and all sky outgoing longwave radiation and absorbed solar radiation are within the order of the error of observation (Kiehl et al., 1996).

The Voight line profile is used to model the radiative cooling in the stratosphere. It incorporates a parameterization of cloud fraction and treatment of cloud optical properties (Kiehl, 1994). It also incorporates a sophisticated treatment of boundary layer processes. It comprises component models of land surface, mixed layer slab-ocean and thermodynamic sea-ice, which are coupled with the atmospheric model. The model also exhibits systematic known biases at the surface and the top of the atmosphere energy budgets. CCM3 incorporates a hydrological cycle well within the magnitude of real observations. It has parameterized convection which includes a simple mass flux representation of moist convection along with deep moist convection formulation. It also incorporates a Sundqvist style evaporation of stratiform precipitation. The land surface component of CCM3 incorporates energy, momentum and carbon dioxide exchanges between the atmosphere and the land. CCM3 also incorporates a hydrostatic matrix and a generalized form of the gravity wave drag parameterization (Kiehl et al., 1996).

B. GCM Simulation and Terra Blanda 3

Modeling the earth's climate and getting data to make statistical deductions requires significantly long runs, which consumes a lot of computing time, with the fact that the length of the run is never enough. The effective heat capacity of the mixed layer of the oceans is about 60 times more than the effective heat capacity of land. Thus, the response time over oceans is much longer than the response time over land. The time scale of the mixed layer ocean model is about five years. To make statistically significant inferences from such a model would require, as a rule of thumb, a run of at least ten times the time scale, about 50 years. The time scale over land is about a month. For an all land planet model, much shorter runs would suffice to make equivalent statistical inferences because of the removal of variables with large time constants attributed to the mixed layer ocean. Thus, one year of an all land planet model is statistically equivalent to 60 years of a mixed ocean layer model in terms of autocorrelation time. By modifying the celestial mechanics, seasons can be removed. Removal of seasons makes each of the months statistically equivalent to the others, removing the annual trend. Thus, another factor of 12 is added to the effective length of the run. Removal of topography leads to a symmetric planet, which means that the two hemispheres are statistically equivalent and every longitude is statistically equivalent to the others. Thus, the effective length of the simulation is further increases by a factor of 2 by pooling data from both the hemispheres.

Overall, the time series obtained from a zonally symmetric, all land planet, running at equinox in a circular orbit is effectively about 1000 times longer than that of a conventional run, that includes geography and seasons. Thus, by running CCM3 on such a planet for 5 years is equivalent to running the conventional model for 5000 years. Running a simulation of 5000 years requires dedicated computer time in the

range of weeks, whereas running the simulation of 5 years on Terra Blanda takes hours. It is emphasized here that the modifications made to the model are only in the geography and the seasonality of the planet. The atmosphere part of the model is untouched, thus the dynamics of the atmosphere remain the same as the conventional model. An all land planet, though unlike earth is a realizable planet whose atmosphere is exactly the same as that of the earth as modeled by CCM3, but whose geography and seasonality are modified to yield effectively longer runs.

An all-land planet model is used in this research, and is termed as Terra Blanda 3. The simulation uses the original NCAR Community Climate Model 3 with modified boundary conditions and solar forcings. Terra Blanda 3 is a simulation of an all land, north-south symmetrical planet, which stays on the equinox throughout the run, and has no non-linearity associated with snow-albedo feedback. The surface of the planet is flat with no topography and vegetation. The oceans and sea-ice are replaced by land. Perpetual equinox was achieved by fixing the obliquity of the model to zero. The eccentricity of the planet was set to zero to remove the annual trend. The reflectivity of snow is set to be the same as that of the rest of the planet, thus removing the snow-albedo feedback mechanism. The land surface is kept at a constant level of soil moisture content, with a wetness factor of 0.25, so that the change in water content does not play a significant role in the dynamics of the model. Thus, we obtain a simulation that returns a stationary time series effectively longer than conventional runs, with data for each longitude statistically equivalent to the other.

Terra Blanda 3 was run for 1500 days, after the climate had settled down to the new boundary conditions. In this experiment, the surface temperature field generated by the model, which is a stationary time series for the model is studied.

CHAPTER IV

BACKGROUND

A. Spectral Transformation

The surface temperature field is used in the experiments performed in this study. The surface temperature field is decomposed into spherical harmonics that serve as basis functions, for most of the experiments. Any periodic field variable on a sphere can be expanded into spherical harmonics in the following way:

$$T(\hat{r},t) = \sum_{n=0}^{N} \sum_{m=-n}^{+n} T_{nm}(t) Y_{nm}(\hat{r}) \tag{4.1}$$

where, Y_{nm} is the spherical harmonic with degree n and zonal wave-number m, and a function of the position vector $\hat{r}$ which is a function of the latitude, θ, the longitude, ϕ and the radius r. The radius on the surface of the earth is assumed to be constant over the entire planet. T_{nm} are the spectral complex coefficients associated with each Y_{nm} at every time step, t (McGuffie and Sellers, 1997).

$$Y_{nm}(\hat{r}) = \sqrt{\frac{(2n+1)(n-m)!}{4\pi(n+m)!}}\ P_n^m(sin\theta)\ e^{im\phi} \tag{4.2}$$

where, P_n^m is a Legendre polynomial of degree n and wave-number m. The spherical harmonics are orthonormal functions, i.e.

$$\int\int_{4\pi} Y_{nm} Y^*_{n'm'}\ d\Omega = \delta_{nn'}\ \delta_{mm'} \tag{4.3}$$

where, Y^*_{nm} is the conjugate of Y_{nm} and Ω is the solid angle. Thus, T_{nm} can be evaluated as follows:

$$T_{nm}(t) = \int\int_{4\pi} Y^*_{nm}(\hat{r})\ T(\hat{r},t)\ d\Omega \tag{4.4}$$

CCM3 uses the standard triangular truncation of degree 42. It is represented spatially, on the sphere, on 64 Gaussian latitudes and 128 equally spaced longitudes, each grid approximately being $2.8^\circ \times 2.8^\circ$. For such a finite grid spherical representation, the values of T_{nm} are evaluated numerically.

B. Stationary Time Series

A univariate time series is defined as a stationary time series if the first and the second moments of the series are independent of time and the covariance between two points in time is only a function of the time lag between the two points.

$$COV\langle T(t),\ T(t')\rangle = f(|t-t'|), \tag{4.5}$$

The Auto-Covariance at lag v is defined as

$$R(v) = \frac{\sum_{t=1}^{n-v}\ (T(t) - \langle T\rangle)(T(t+|v|) - \langle T\rangle)}{n} \tag{4.6}$$

where, n is the length of the time series, $\langle\ T\ \rangle$ is the mean of the variable T. And, the Auto-Correlation function, ρ at lag v is defined as

$$\rho(v) = \frac{\sum_{t=1}^{n-v}\ (T(t) - \langle T\rangle)(T(t+|v|) - \langle T\rangle)}{\sum_{t=1}^{n-v}\ (T(t) - \langle T\rangle)^2} \tag{4.7}$$

The sample Auto-Correlation Time is taken to be the value of lag, v for which

$$\rho(v) = \frac{\rho(0)}{e} \tag{4.8}$$

C. Spatial Correlation and Length Scale

Correlation between two random variables X and Y having values $x_1, x_2, x_3, \ldots, x_n$ and $y_1, y_2, y_3, \ldots, y_n$ respectively, is defined as

$$CORR(X,Y) = \frac{\sum_{i=1}^{n} (x_i - \bar{x})\ (y_i - \bar{y})}{\sqrt{\sum_{i=1}^{n} (x_i - \bar{x})^2\ \sum_{i=1}^{n} (y_i - \bar{y})^2}} \tag{4.9}$$

To evaluate the length scale, spatial correlation is used in this study. Time series of the daily average surface temperature was obtained for each of the grid points on Terra Blanda for 1510 days of simulation. The surface temperature time series of each grid point is considered as a random variable. A test site is then identified to study its spatial correlation. The surface temperature time series at the test site is correlated with each of the neighboring grid points. The correlations thus obtained are plotted as contours to obtain the spatial correlation plot.

Length scale is defined as the distance at which the correlation of a variable falls to 1/e from the test point. Thus, the length scale for the surface temperature field is evaluated as the average distance of the 1/e level contour from the test site. Hansen and Lebedeff (1987) found length scales in the range of 1700 km in mid and polar latitudes. They measured the correlation of annually averaged temperature data at various stations around the globe. North (1984) used the EBM to suggest a length scale in the range of 1000-2000 km for the temperature field on the earth. North et al. (1992) used Terra Blanda to evaluate the length scale to be in the same range. Here, various test points are considered on Terra Blanda 3. Correlations with the neighboring points are evaluated at each of these points. These correlations are plotted and observed to determine the length scale.

D. Variance Distribution

Variance of a random variable, T is defined as

$$\sigma_T^2 = \frac{\sum_{i=1}^{n} (T_i - \bar{T})^2}{n-1} \tag{4.10}$$

The temperature field is represented by spherical harmonic basis functions. For every spherical harmonic degree n, there are $2n + 1$ longitudinal modes. The distribution of variance in each of the spherical harmonic degree is not equal (North et al., 1992). The lower modes have more power, which increases linearly till degree 8, and then reduces exponentially. This is observed in the distribution plot. Variances of each of the modes of a degree are evaluated over the 1510 days run. These variances are summed to obtain the variance of a spherical harmonic degree. The over turn at degree 8 can be explained by the eddy flows. Large atmospheric waves exist in the earth climate system, and travel around the earth. However, smaller waves cannot travel across the earth, and fizzle out. This fizzling out starts at modes 8 and higher, after which the waves are more like eddies and die out quickly. Thus, the higher modes do not contribute much to the variance of the temperature field.

E. Auto-Regressive Processes of Degree 1 (AR1)

An auto regressive process, X of degree 1 is defined as

$$X(t) = \lambda X(t-1) + \epsilon(t) \tag{4.11}$$

where, ϵ(t) is white noise. And, Auto-Correlation Time, τ can be evaluated from the value of lambda as

$$\tau = \frac{1}{1-\lambda} \tag{4.12}$$

F. Spectral Density

A discrete univariate periodic function of n points can be expressed as a sum of $n/2$ harmonic functions and can be expressed in terms of cosines and sines as:

$$Y(t) = A_0 \ + \sum_{k=1}^{n/2} \left\{ A_k \cos\left[\frac{2\pi kt}{n}\right] \ + \ B_k \sin\left[\frac{2\pi kt}{n}\right] \right\} \tag{4.13}$$

where, $k/n = f$, the frequency and A_k and B_k are coefficients. The above is known as the Fourier expansion. Each frequency has a definite intensity associated with it that explains the amount of variability of the function. The spectral line intensity of a particular frequency is defined as :

$$C_k^2 = A_k^2 + B_k^2 \tag{4.14}$$

A plot of C against the frequency domain is known as the spectrum of the univariate function. The spectrum can be normalized to obtain the normalized spectral density of the function.

$$R^2 = \frac{n/2C_k^2}{(n-1)\sigma^2} \tag{4.15}$$

R_k^2 and C_k^2 are chi-squared distributed with two degrees of freedom, as they are the sum of squared terms A_k and B_k, which are both normally distributed.

G. Smoothing

The statistical characteristics of a sample are not the same as that of the whole population. In this study the surface temperature field of Terra Blanda 3 is studied for a finite number of days, and thus the characteristics of the sample of data considered is prone to sampling errors. One way to evaluate the sampling error of the spectrum of a time series where the low frequencies are of interest, is to smooth the spectral

density by a simple moving average, with a bandwidth b, i.e

$$R_{ks}^2 = \frac{1}{b} \sum_{i=k-b/2}^{k+b/2} R_i^2 \tag{4.16}$$

For a white noise spectrum the standard error associated with the moving average smoother is given by $\sigma/\sqrt{2b}$. Thus, the 90% confidence interval of the sample spectrum can be plotted, but the sampling error of the spectral line intensity is dependent on the frequency. For, a chi-square distribution, the standard deviation is equal to the mean, thus, if a log-linear scale is used to plot the spectral density, the sampling error bar appears to be the same over the entire plot range. The above method for the white noise spectrum can approximately be applied to somewhat skewed spectrum such as the surface temperature data in this study.

H. Green's Function

North and Cahalan (1981) and North et al. (1992) stated that for a one dimensional energy balance model with constant diffusion over all latitudes, the influence function of the surface temperature field at one point on another can be expressed by the Greens function as follows

$$\Delta T = g \sum_{n=0,2,\ldots}^{N} \frac{(2n+1)P_n(\sin(\theta))P_n(\sin(\theta'))}{n(n+1)D + B} \tag{4.17}$$

where, $P_n(\sin(\theta))$ is the legendre polynomial in $\sin(\theta)$, the sine of the latitude of the point of study and $P_n(\sin(\theta'))$ is the legendre polynomial in $\sin(\theta')$, the sine of the latitude of the causal point. N is the truncation level. D is the thermal diffusion coeffcient and B is the radiation damping term. North et al. (1992) took the values of D to be 0.2 (earth radius)$^{-2}$W$(^{\circ}C)^{-1}$ and B to be 2.0 W $m^{-2}(^{\circ}C)^{-1}$ for their comparison of the EBM with CCM0, and g is the scaling factor that is equivalent to

the magnitude of the forcing at the causal point. The values of D and B used in this study are the same as those used by North et al. (1992) for the sake of comparison.

I. Generalized Extreme Value Distributions

The extreme value theory states that the distribution of

$$M_n = maximum(x_1, x_2, \ldots, x_n) \tag{4.18}$$

where $(x_1, x_2, \ldots x_n)$ is a block of a sequence of independent random variables having any common distribution, is a distribution function of the form

$$G(z) = \exp\left\{-\left[1 + \xi(\frac{z-\mu}{\sigma})\right]^{-\frac{1}{\xi}}\right\} \tag{4.19}$$

where, μ is the location parameter, σ is the scaling parameter and ξ is the shape factor. These parameters can be estimated by using the maximum log-likelihood method (Coles, 2001). In this study, the above stated theory is applied on the simplified AR1 model fit of the surface temperature field data obtained from Terra Blanda 3 to comprehend the extreme values of the field.

CHAPTER V

RESULTS AND COMPARISONS WITH CCM0

CCM3 is run on Terra Blanda 3 for 1500 days after statistical equilibrium is established. The surface temperature field is extracted from the model run, and decomposed into spherical harmonics. These spherical harmonics components are then used to evaluate the length-scale, time-scale, auto-correlation time, and study the response to various forcings. Leung and North (1991) and North et al. (1992) applied CCM0 to Terra Blanda and performed similar studies. A comparison of the results obtained from the two models is conducted here. For the sake of clarity, we refer to the idealized planet used earlier with CCM0 as Terra Blanda, and Terra Blanda 3 is used when referring to the idealized planet created for this study on which CCM3 is applied. The surface temperature field is used as the basis of comparison, as it has been the variable under study for both the models. Figure 1 and Fig. 2 show the long term zonal mean temperature of Terra Blanda and Terra Blanda 3 both running at equinox. The profile of Terra Blanda shows a strong temperature gradient in the tropics, which is in contrast with the real world. The temperature gradient in the tropics of Terra Blanda 3 is flatter than that of Terra Blanda, thus being closer to the real world, possibly indicating the greater complexity of CCM3.

The variance of the zonal average temperature is expected to be greater at high latitudes because of the reduction of the number of independent spatial samples averaged around a zone near the poles. This can be explained by the geometry of the sphere (Leung and North, 1991). The number of longitudinal grids at the polar region is the same as that at the equator or the mid-latitudes, however the distance between two longitudinal grids is much less at the poles than at other latitudes. Based on the spatial correlation plot, the temperature at a point is correlated to a point 1000-2000

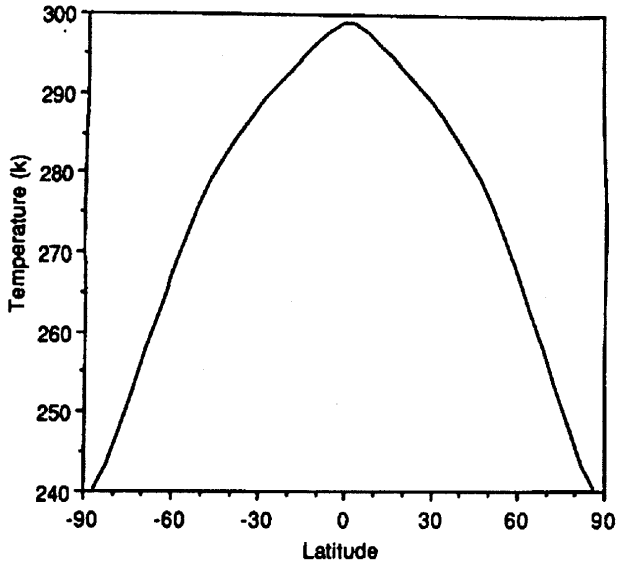

Fig. 1. Zonally averaged temperature over different latitudes on *Terra Blanda*. (Leung and North, 1991)

km from it, thus the number of independent samples in polar regions is less than that at other latitudes and the variance is greater. Figure 3 and Fig. 4 show the time variance of zonal averaged temperatures on Terra Blanda and Terra Blanda 3. Both exhibit increasing variance from the mid-latitudes to the poles. The length scale is derived from the spatial-correlation of a test point with neighboring points. For Terra Blanda 3, for the mid-latitudes, the length scale is found to be 1200 km with notable isotropy. For the polar region, it is found to be 1000 km, and for the equator, it is estimated to be 1700 km. Figure 5 and Fig. 6 show the spatial correlation plot of Terra Blanda and Terra Blanda 3 at the mid-latitudes. Figure 7 and Fig. 8 show the spatial correlation plot of Terra Blanda and Terra Blanda 3 near the equator. The spatial correlations obtained on Terra Blanda by North et al. (1992) are somewhat isotropic and the length scales obtained are in the range of 1000-2000km and are similar to that obtained for Terra Blanda 3. Figure 9 shows the plot for the polar

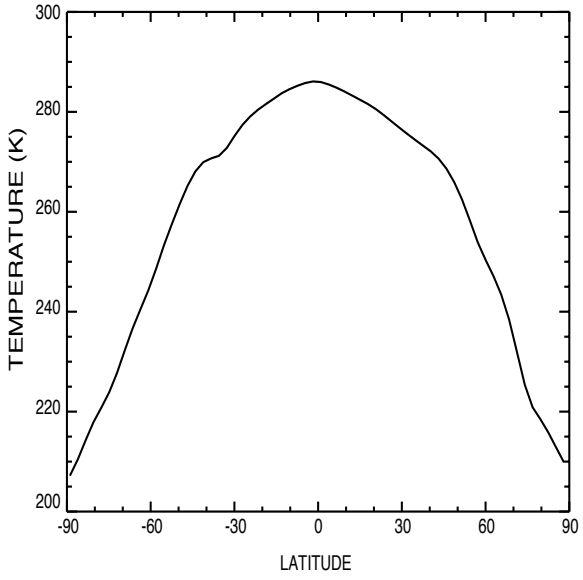

Fig. 2. Zonally averaged temperature over different latitudes on *Terra Blanda 3*

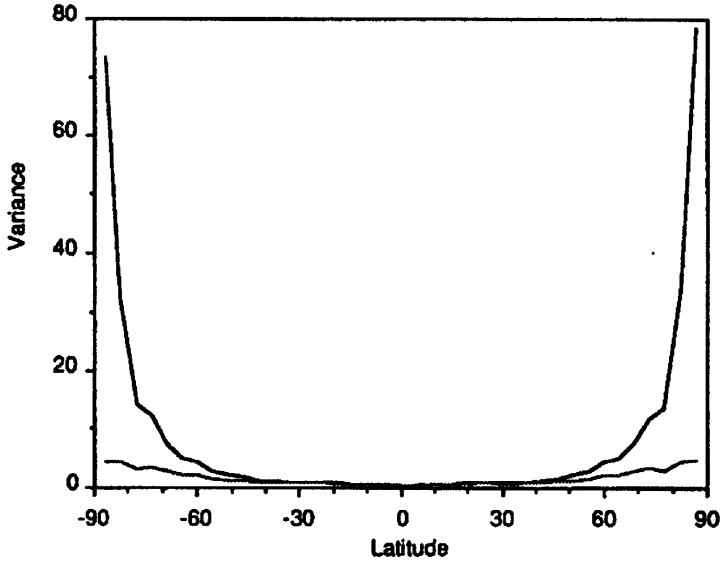

Fig. 3. Variance of the zonally averaged temperature over different latitudes on *Terra Blanda* (Leung and North, 1991).

regions on Terra Blanda 3.

The variance distribution graph is plotted corresponding to each of the spherical harmonic degrees. Figure 10 and Figure 11 show the variance distribution of the surface temperature as a function of the spherical harmonic degree for Terra Blanda and Terra Blanda 3 respectively. There is a maximum at degree 8 and a break in the slope of the curve at degree 15 for Terra Blanda because of the rhomboidal truncation at degree 15. The variance distribution plot obtained from Terra Blanda 3 is similar to the one obtained by North et al. and is linear up to degree 8, and it then decreases without any breaks. Thus, implying that the triangular truncation used in CCM3 provides a smooth variance distribution curve at higher spherical harmonic degrees.

The surface temperature field is decomposed into spherical harmonic functions, and the time series is obtained for the spherical harmonic coefficients T_{00}, T_{20} and T_{40}. T_{00} is directly proportional to the global average temperature. The auto-correlation

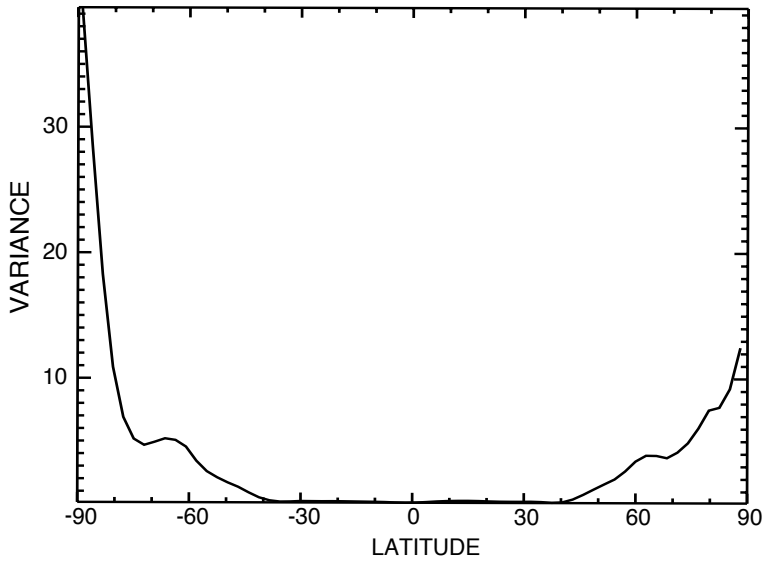

Fig. 4. Variance of the zonally averaged temperature over different latitudes on *Terra Blanda 3*

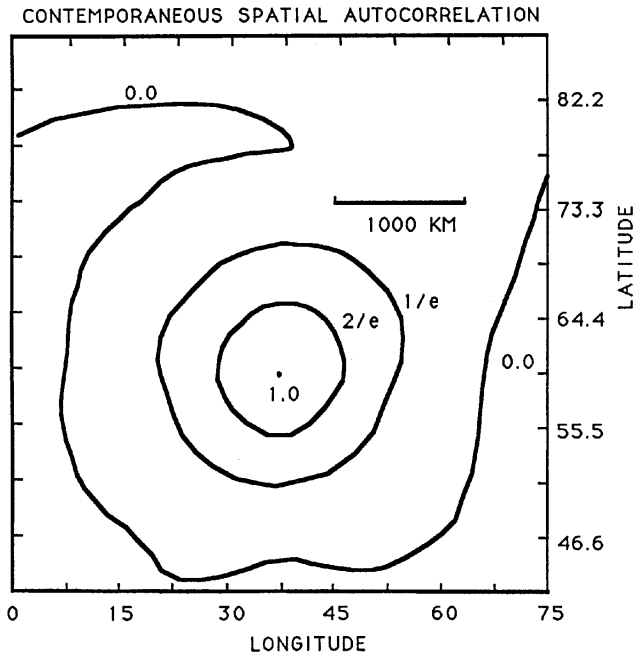

Fig. 5. Spatial auto-correlation of the surface temperature field of a test point in the mid-latitudes with neighboring points on *Terra Blanda* (North et al., 1992).

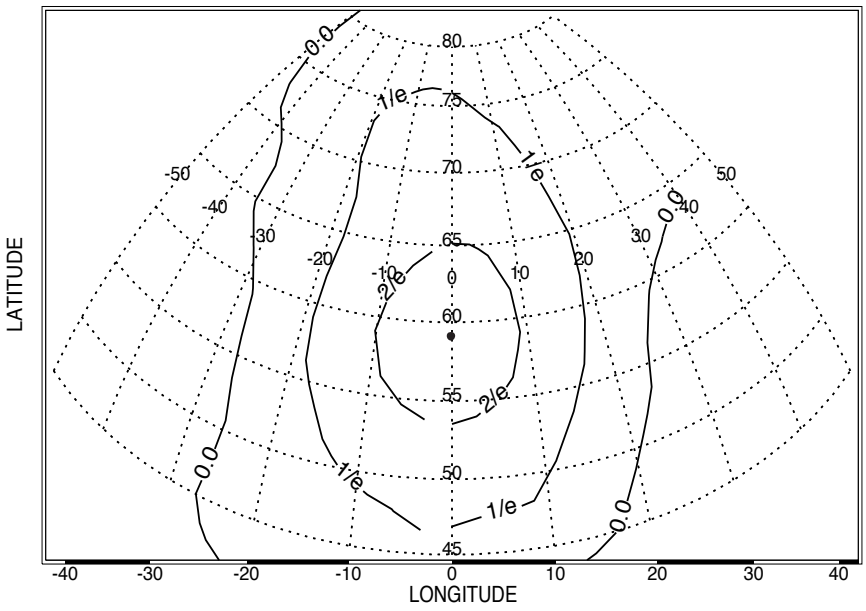

Fig. 6. Spatial auto-correlation of the surface temperature field of a test point in the mid-latitudes with neighboring points on *Terra Blanda 3* using the azimuthal method of map projection

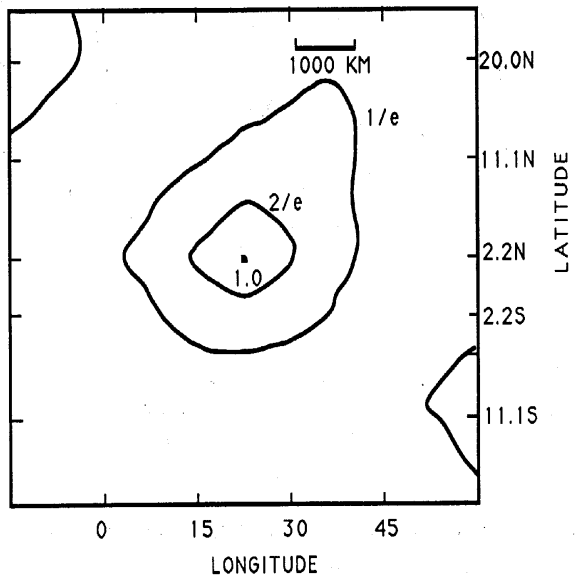

Fig. 7. Spatial auto-correlation of the surface temperature field of a test point near the equator with neighboring points on *Terra Blanda* (North et al., 1992).

functions of the spherical harmonics coefficients T_{00}, T_{20} and T_{40} for the 1510 day run on Terra Blanda 3 are plotted. The time period at which the auto-correlation drops to $1/e$ is considered to be the auto-correlation time and the time scale of this spherical harmonic coefficient. On Terra Blanda 3, for T_{00}, the auto-correlation time is found to be 24 days. For T_{20} and T_{40} it is found to be 10 and 8 days respectively on Terra Blanda 3. Figure 12 and Figure 13 show the autocorrelation functions for T_{00}, T_{10} and T_{20} for Terra Blanda obtained by North et al. (1992) for a dry Terra Blanda with no soil moisture and a wet Terra Blanda with a wetness factor of 0.75 and In this study, a wetness factor of 0.25 is used.

The auto-correlation functions for Terra Blanda 3 are shown in Figure 14. The auto-correlation times obtained for Terra Blanda 3 are between that obtained for the dry Terra Blanda and the wet Terra Blanda. Thus, it is seen that the addition of water plays a significant role in the energy balance of the system and effects the time

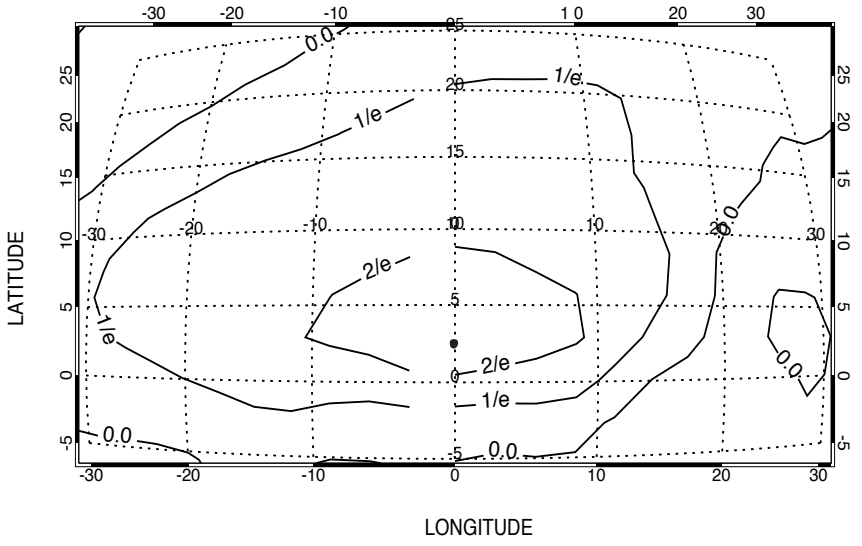

Fig. 8. Spatial auto-correlation of the surface temperature field of a test point at 1.9°N with neighboring points on *Terra Blanda 3* using the azimuthal method of map projection.

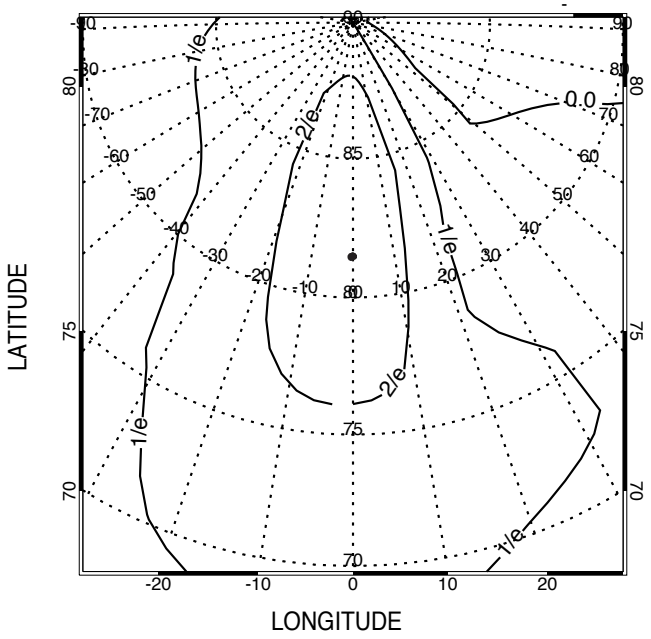

Fig. 9. Spatial auto-correlation of the surface temperature field of a test point at 81.6°N with neighboring points on *Terra Blanda 3* using the azimuthal method of map projection.

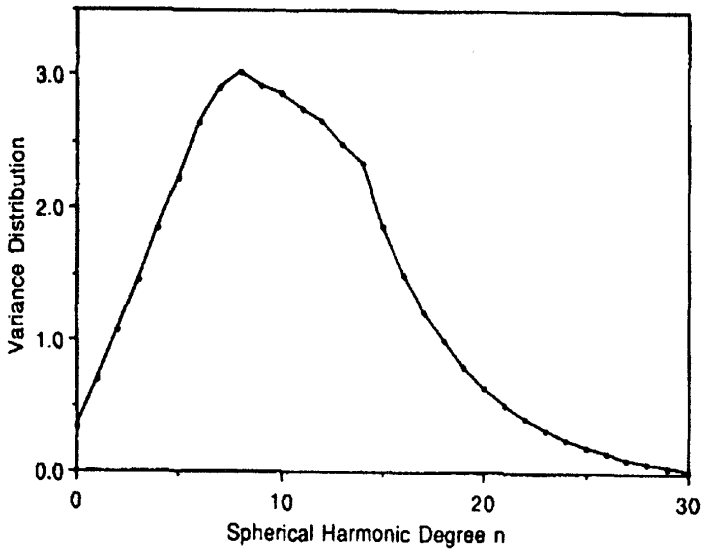

Fig. 10. Variance of the surface temperature as a function of spherical harmonic of degree n for *Terra Blanda* (Leung and North, 1991).

scale.

Spectral analysis is performed on the spherical harmonics coefficients T_{00}, T_{20} and T_{40}. Figure 15 and Figure 16 show the spectral density of T_{00}, T_{20} and T_{40} for Terra Blanda and Terra Blanda 3. The smoothing bandwidth used for the Terra Blanda 3 plots are too small to be shown, but the confidence intervals associated with the smoothing are shown. To show the resemblance of the behavior of these coefficients, theoretical AR1 processes having auto-correlation times and variances equal to the auto-correlation times and variances of the corresponding spherical harmonic coefficients are also shown. These figures validate that the AR1 processes can still be used to model some aspects of the surface temperature field, in spite of the complexities associated with CCM3.

In the simulation, a sinusoidal solar forcing is applied to CCM3. The solar insolation is made to vary sinusoidally with a period of 30 days and an amplitude

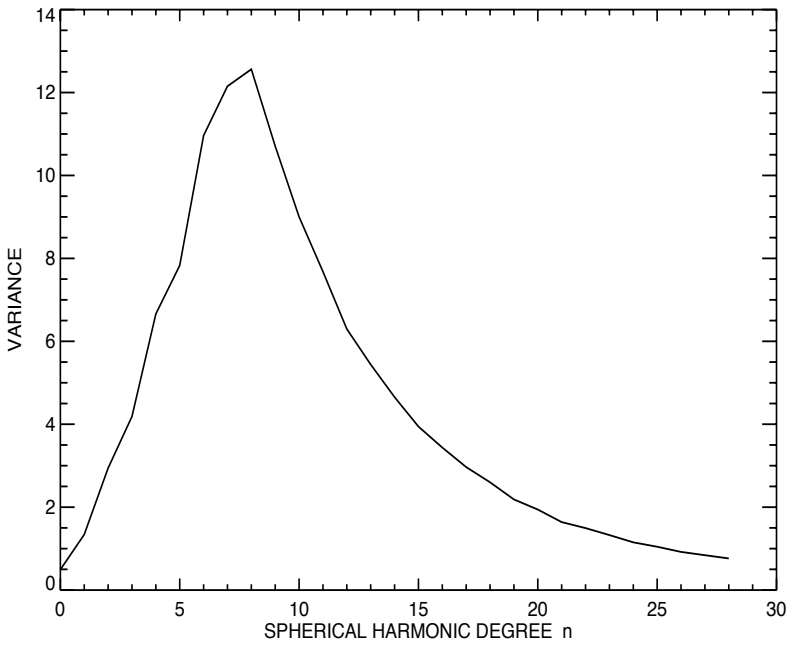

Fig. 11. Variance of the surface temperature as a function of spherical harmonic of degree n for *Terra Blanda 3*.

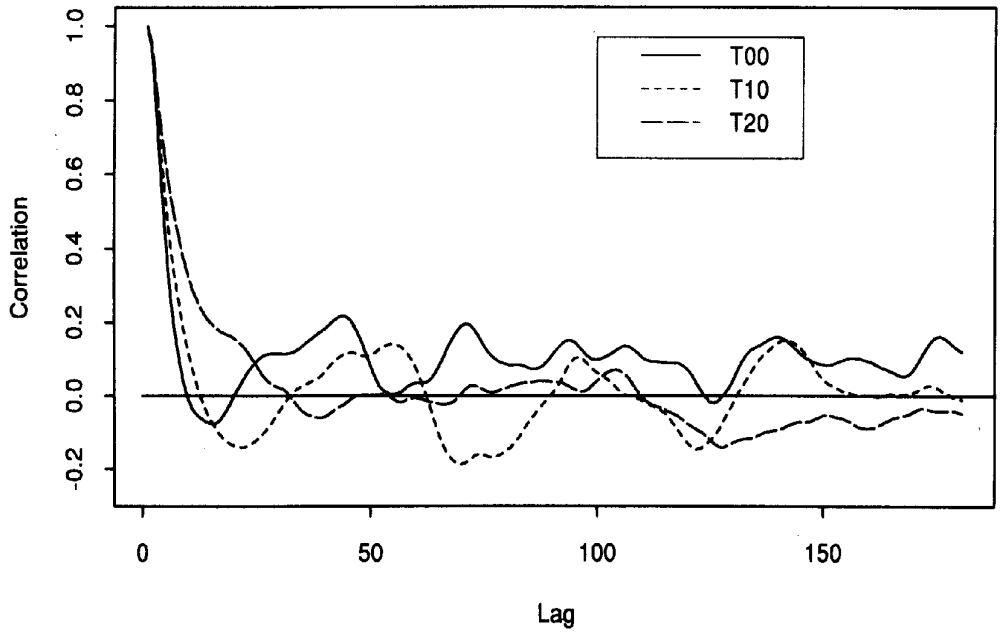

Fig. 12. Auto-correlation functions of T_{00}, T_{10}, T_{20} on a dry *Terra Blanda* (North et al., 1993).

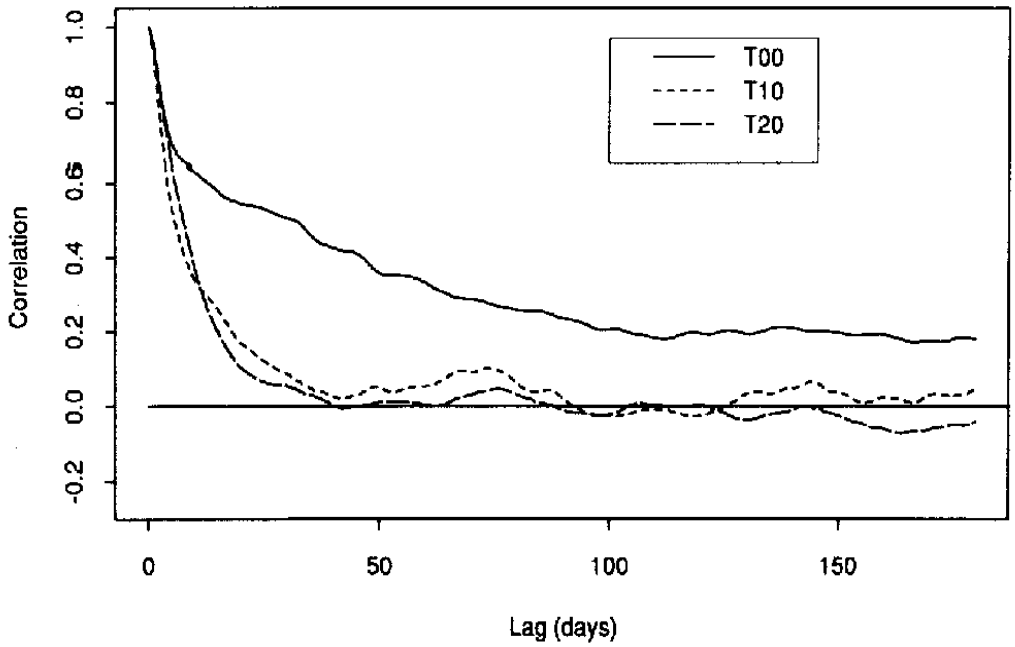

Fig. 13. Auto-correlation functions of T_{00}, T_{10}, T_{20} on a wet *Terra Blanda* (North et al., 1993).

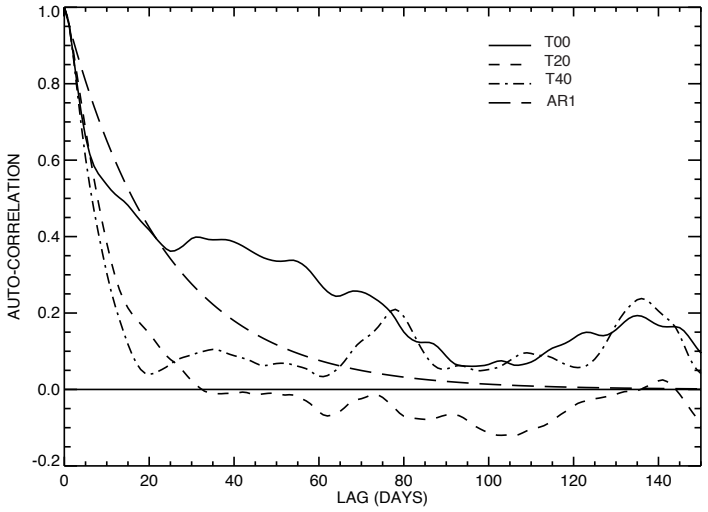

Fig. 14. Auto-correlation functions of T_{00}, T_{20}, T_{40} on *Terra Blanda 3* and an AR1 process of auto-correlation time of 24 days.

of 20% for 300 days. The response of the surface temperature field is studied. The resulting surface temperature field is decomposed into its spherical harmonic basis functions. The spectral densities of the resulting spherical harmonic coefficients T_{00}, T_{20} and T_{40} are plotted. All the plots show a significant peak at the 30 days period, same as the period of forcing. Peaks are not visible at the harmonics of this period, i.e. at periods of 15, 10 or other harmonics of 30. Figure 17 and Fig. 18 show the spectral density plots of T_{00}, T_{20} and T_{40} obtained from Terra Blanda (North et al., 1992) and Terra Blanda 3 in response to a sinusoidal solar forcing with a period of 30 days and amplitude of 20%. Peaks are observed at a frequency corresponding to 30 days time period, insinuating on the linearity of response for both the models. There are no significant peaks at other harmonics of 30 days, for both Terra Blanda and Terra Blanda 3 for the 20% amplitude, implying that the response to large forcings is fairly linear for CCM3 too. North et al. (1992) showed that this linearity breaks

for higher amplitudes for CCM0. They observed the appearance of peaks at time periods of 15 days and 10 days in the spectral density plot of the response of the surface temperature field to a sinusoidal solar forcing of amplitude of 40% with a time period of 30 days on Terra Blanda.

Another experiment to test the linearity of response is to place a latitudinal ring heat source and study the response of the surface temperature field. A latitudinal ring heat source of 50 W/m^2 at 60° North and South on Terra Blanda is created by adding 50 W/m^2 of flux to the radiative long wave upward flux at the surface on a 15° wide band centered at 60° North and South each. The model with such a forcing is run for 50 autocorrelation times of the global average surface temperature. The response of the surface temperature to a zonal heat forcing is studied by comparing it with the situation when no heat source was placed. Zonal average temperature is calculated at each of the latitudes for both the situations. The difference of these climatologies is termed the influence function. The influence function is plotted to analyze the effect of the zonal forcing. Peaks are observed at the corresponding heat source centers namely 60° North and South. Overall, the surface temperature of Terra Blanda rises. Figure 19 shows the response of the surface temperature field to a 15° wide zonal heat latitudinal ring of 50 W/m^2 on Terra Blanda located at 60° North and South (North et al., 1992).

There is a peculiar behavior of the zonal influence function curve on Terra Blanda, as it shows warming at the poles. North et al. (1992) noted that this strange response at the poles was due to the rhomboidal truncation of degree 15 used in CCM0. Figure 20 shows the response to an exact same forcing applied on Terra Blanda 3. Both these graphs also show the influence function of the EBM obtained by using the Green's function (eqn. 4.20) for various degrees of truncation. As expected, the peculiar warming at the poles dies down, owing to the triangular truncation of degree

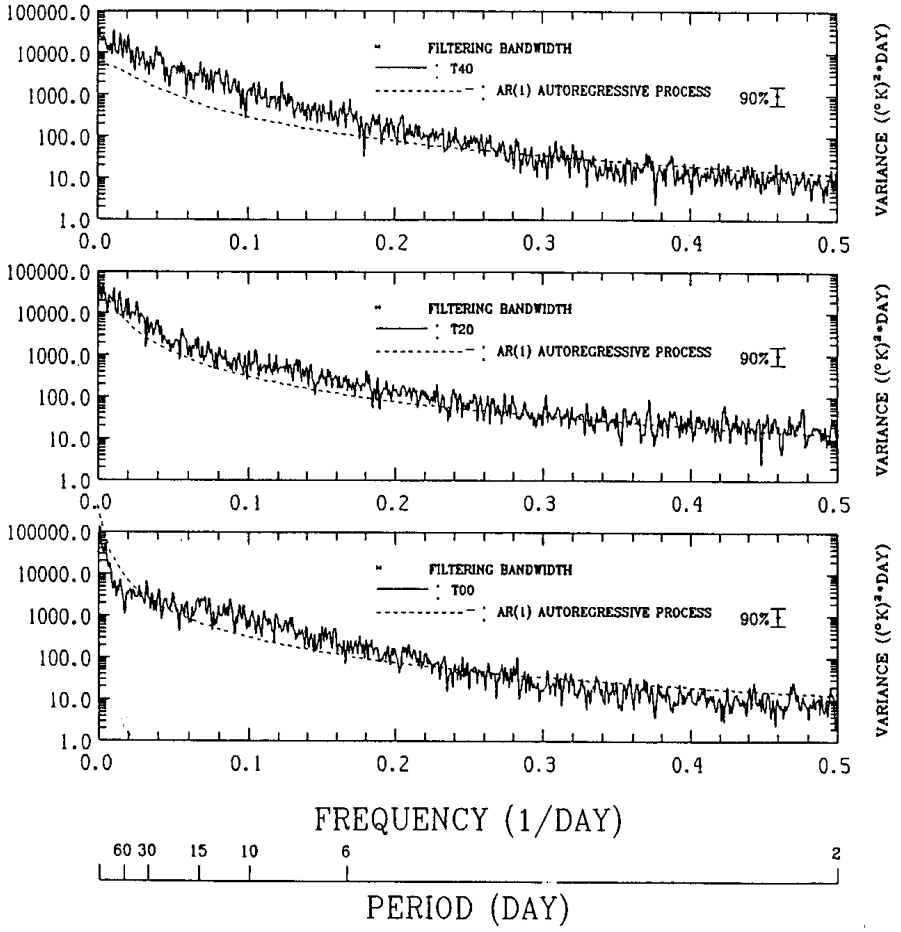

Fig. 15. Logarithms of the smoothed spectral density of spherical harmonic coefficients T_{40}, T_{20} and T_{00} for *Terra Blanda* (North et al., 1992).

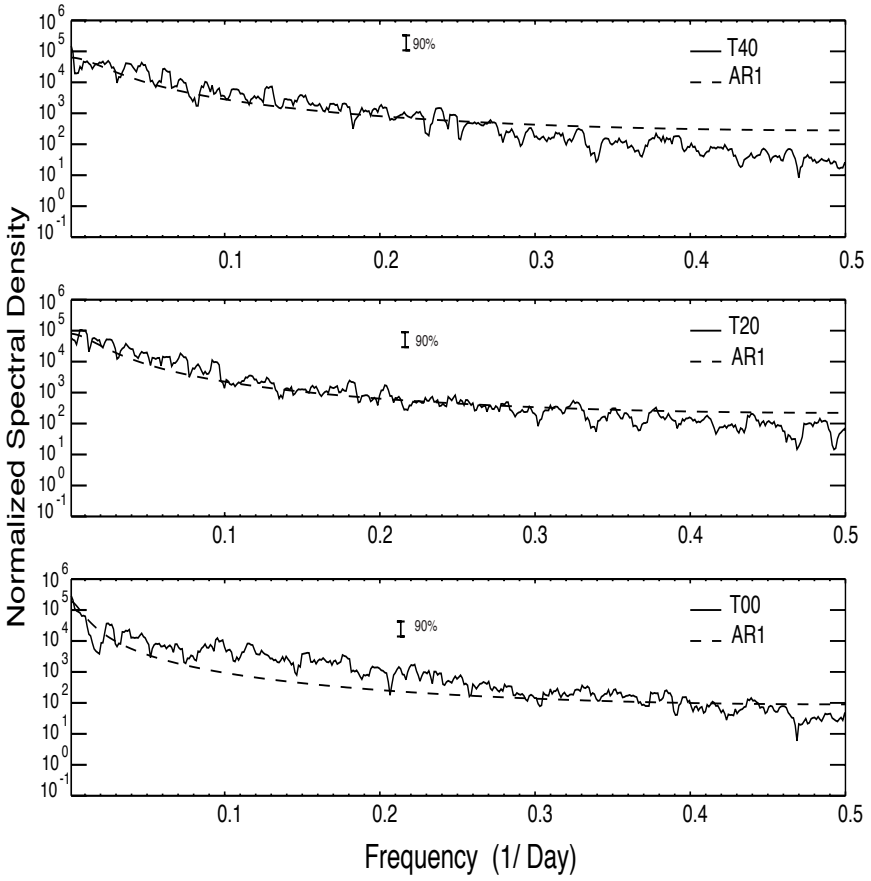

Fig. 16. Logarithms of the smoothed spectral density of spherical harmonic coefficients T_{40}, T_{20} and T_{00} for *Terra Blanda 3*.

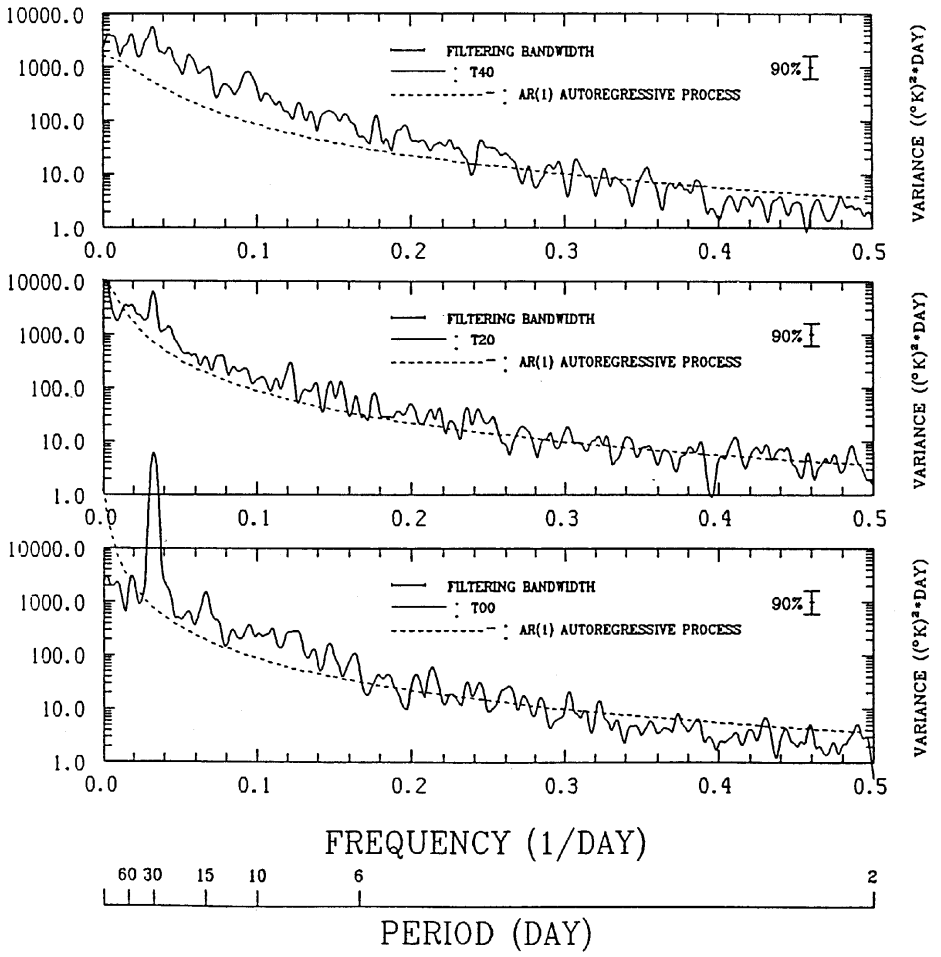

Fig. 17. Logarithms of the smoothed spectral density of spherical harmonic coefficients T_{40}, T_{20} and T_{00} for *Terra Blanda* in response to a 20% sinusoidal variation of the solar constant with period 30 days (North et al., 1992).

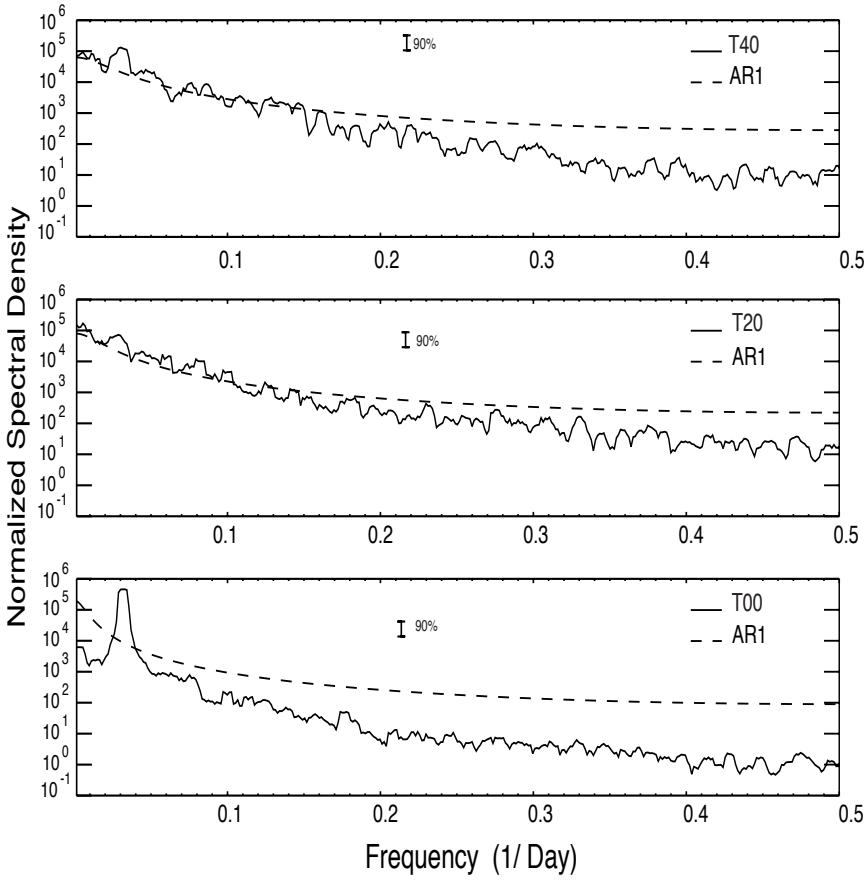

Fig. 18. Logarithms of the smoothed spectral density of spherical harmonic coefficients T_{40}, T_{20} and T_{00} for *Terra Blanda 3* in response to a 20% sinusoidal variation of the solar constant with period 30 days.

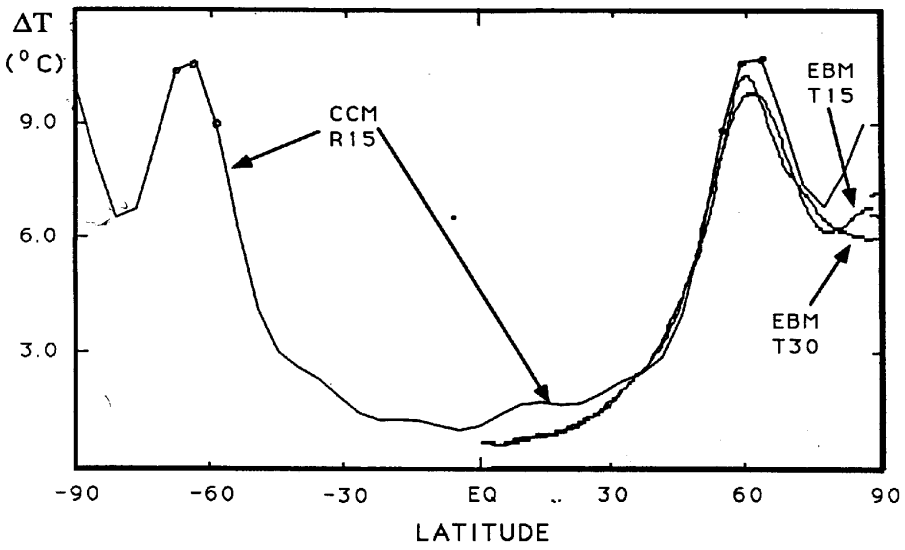

Fig. 19. Influence function for a 15° wide band of heat source centered at 60°N and 60°S on *Terra Blanda* along with influence function of EBM truncated at Legendre polynomial degree 15 and degree 30 (North et al., 1992).

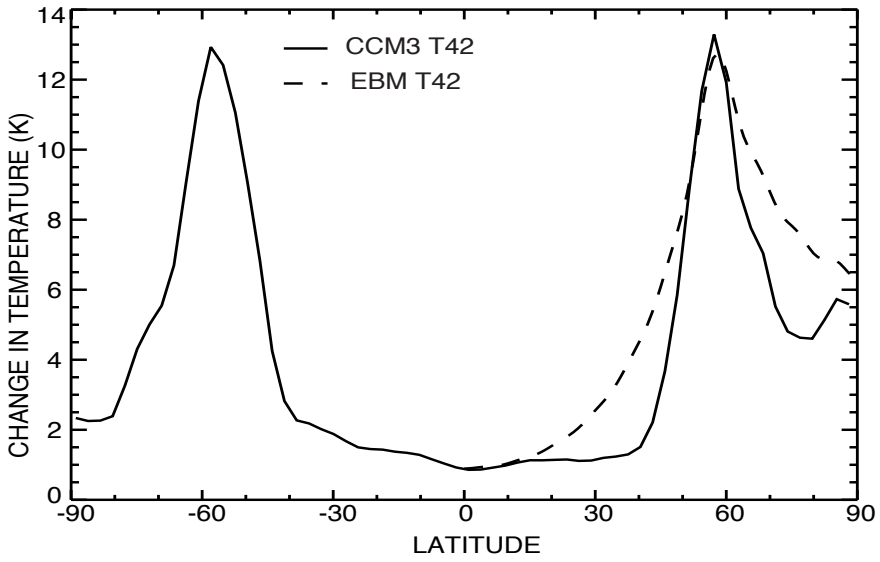

Fig. 20. Influence function for a 15° wide band of heat source centered at 60°N and 60°S on *Terra Blanda 3* along with influence function of EBM truncated at Legendre polynomial degree 42.

42 used in CCM3. A difference noted in the two plots from Terra Blanda and Terra Blanda 3 is the flattening of the zonal influence function near the tropics for Terra Blanda 3, possibly implying the presence of a more prominent Hadley cell in CCM3 as compared to CCM0. The above also implies that the length scale at the mid-latitudes of CCM3 on Terra Blanda 3 is shorter than that of the EBM and CCM0. Another subtlety worth mentioning here is that the EBM and CCM0 are much more alike, than are CCM3 and EBM, again emphasizing on the complexity of CCM3 over CCM0. Figure 21 shows the average of the two hemispheres, thus increasing the sample size of the data to get a more accurate plot. There is little sign of warming at the poles, which may be attributed to the greater variablity there. Exactly similar experiments are conducted but with a heat sources of 5 W/m^2 and 30 W/m^2 on Terra Blanda 3. The average response of the zonal average temperature at 60° North and South to each of these forcings is plotted against the amplitude of these forcings to check the linearity of response. Also, shown are the error bars associated with each response to the forcings. Figure 22 shows that the plot is nearly a straight line implying that the surface temperature increases linearly with the increase in the amplitude of zonal forcing.

To test the applicability of Fluctuation Dissipation Theory to CCM3 as applied to Terra Blanda 3, the decay of naturally occurring anomalies is compared with that of the response of external forcings and the autocorrelation function of the temperature field. To create a sub-ensemble of decaying natural anomalies, the time series of global average surface temperature is scanned for anomalies greater than 2 standard deviations from the mean. When such an anomaly is found a sub-ensemble member is made out of the time series starting at the occurrence of the anomaly to two auto-correlation times of the global average surface temperature. The sub-ensemble thus

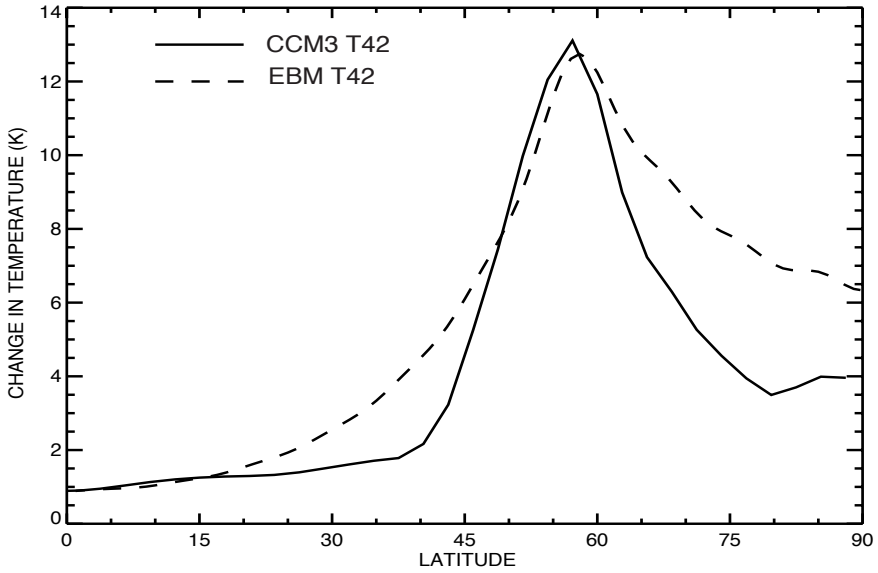

Fig. 21. Influence function for a 15° wide band of heat source centered at 60°N and 60°S on *Terra Blanda 3* averaged over the two hemispheres along with influence function of EBM truncated at Legendre polynomial degree 42.

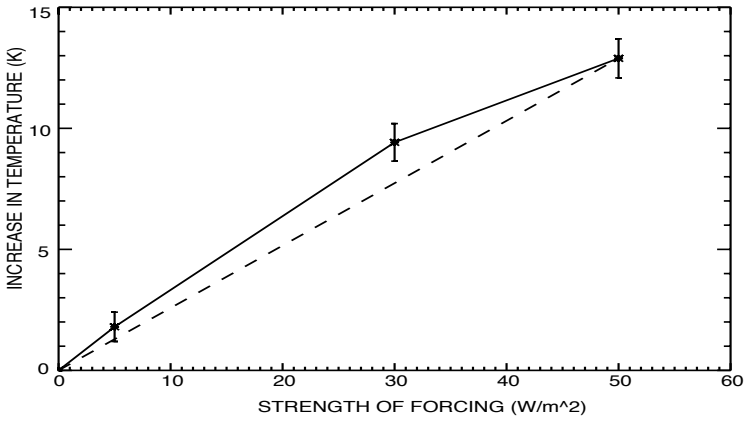

Fig. 22. Amplitude of response at the center of the ring heat source versus the amplitude of the ring heat source on *Terra Blanda 3*.

created is averaged and normalized. Normalization is done by the following method:

$$N(t) = \frac{T(t) - \langle T \rangle}{T(0) - \langle T \rangle} \tag{5.1}$$

Where, N is the normalized value, t is the lag from the occurrence of the anomaly, T is the mean temperature of the sub-ensemble, t is the time after the occurrence of the anomaly.

The external forcing, that is applied, to compare with the sub-ensemble of naturally occurring anomalies, is a step function of solar insolation. Solar insolation is increased by 4% suddenly on Terra Blanda 3 on 5 occasions. These runs are separate from the 1510 days run and are uncorrelated to each other. Different points in time are chosen to increase the solar forcing to obtain an ensemble. North et al. (1993) conducted a similar experiment on Terra Blanda. The response of the step function solar insolation increase is shown in Fig. 23 for Terra Blanda 3 on one of these occasions. These responses are normalized and inverted for Terra Blanda 3. Figure 24 shows the inverted normalized ensemble of the response of the five simulations. The inverted normalized responses are then averaged and plotted to obtain the mean step function response curve, which is then compared with the normalized curve of the sub-ensemble of the decay of the naturally occurring anomalies. These two normalized curves and the autocorrelation function of the global average temperature are plotted together for the purposes of qualitative comparison. Figure 25 and Fig. 26 show the normalized decay of anomalies and the auto-correlation function for T_{00} for the dry and wet Terra Blanda (North et al., 1993). Similarly, Figure 27 and Fig. 28 show the normalized response of step function solar forcing of 4% and the auto-correlation function for dry and wet Terra Blanda (North et al., 1993). Figure 29 shows the decay of naturally occurring 2 σ anomalies, the inverted normalized response to the step function 4% increase of the solar constant and the auto-correlation function.

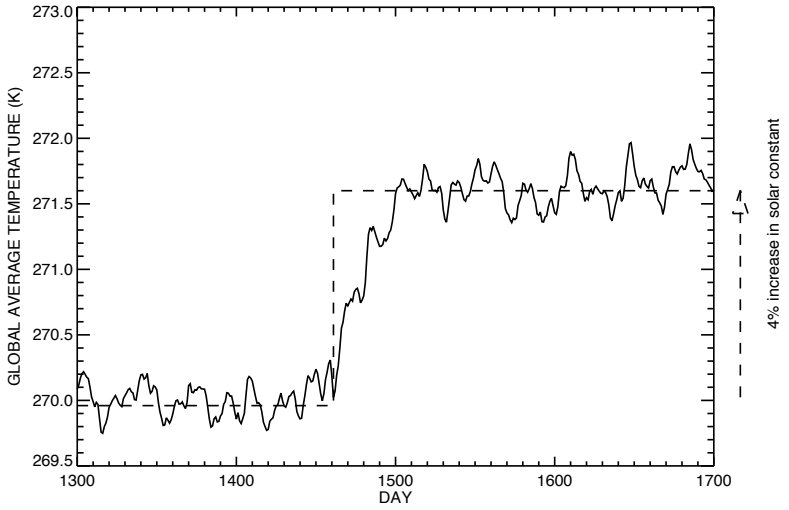

Fig. 23. Response of the global average surface temperature field to the step function forcing of 4% increase is solar constant on *Terra Blanda 3*

It is noted from the plots from Terra Blanda 3 that the normalized decay of anomalies and the auto-correlation function match each other better than Terra Blanda. It is also observed that the relation between the response to step function solar forcing and the auto-correlation is more prominent for Terra Blanda 3.

These plots show that there is a remarkable similarity in all the three situations, implying that the Fluctuation Dissipation Theorem somewhat holds for CCM3 as applied to Terra Blanda 3, and is better validated for CCM3 than for CCM0.

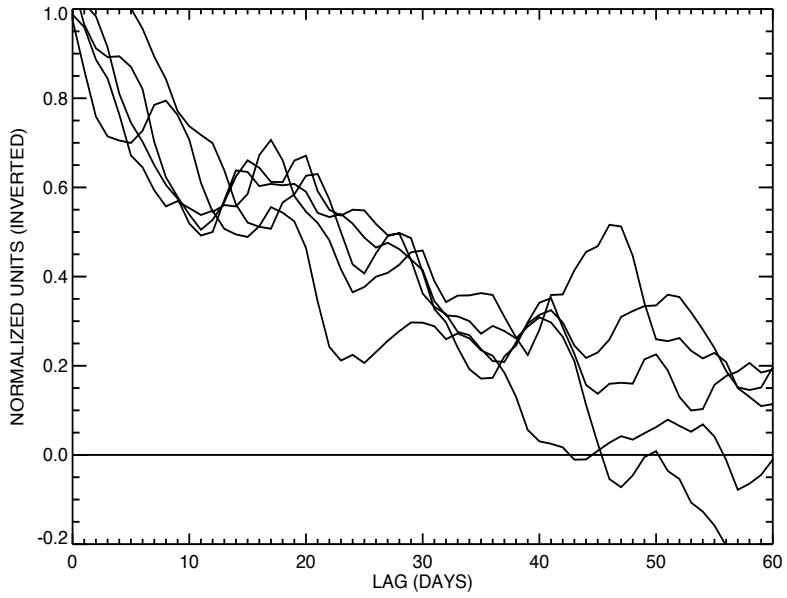

Fig. 24. Ensemble of the inverted normalized response curve of 5 simulations of the step function increase of the solar constant

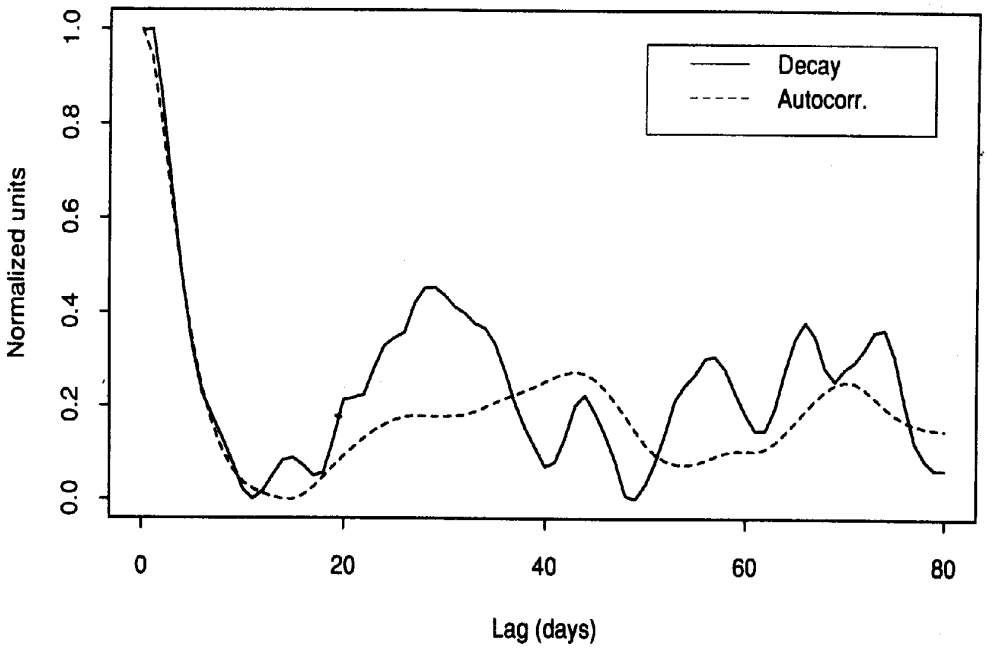

Fig. 25. Decay of the 2σ naturally occurring anomalies in T_{00} and the auto-correlation function of T_{00} on a dry *Terra Blanda* (North et al., 1993).

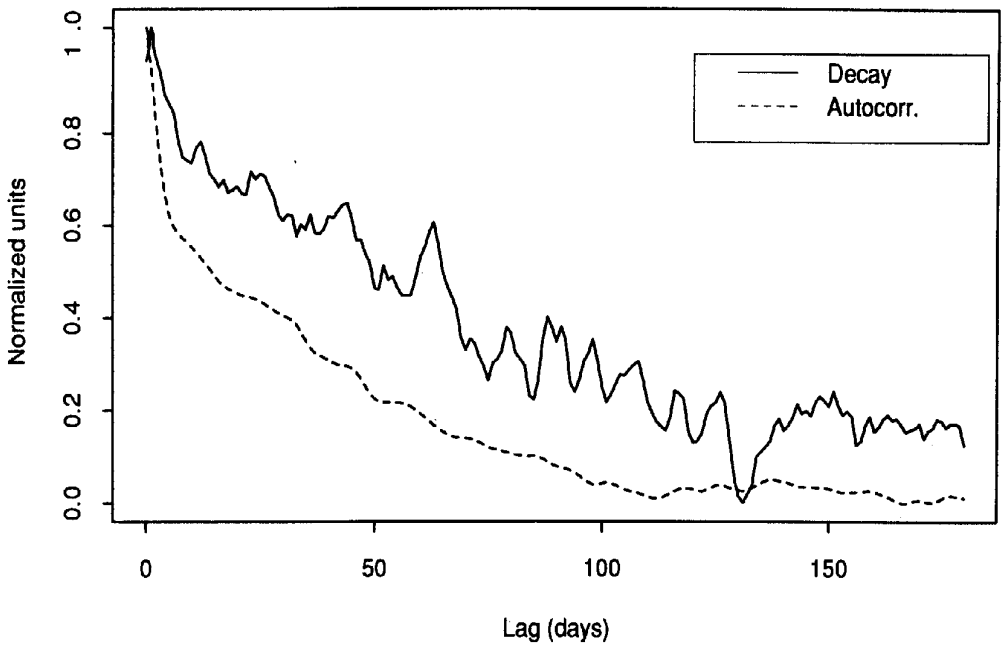

Fig. 26. Decay of the 2σ naturally occurring anomalies in T_{00} and the auto-correlation function of T_{00} on a wet *Terra Blanda* (North et al., 1993).

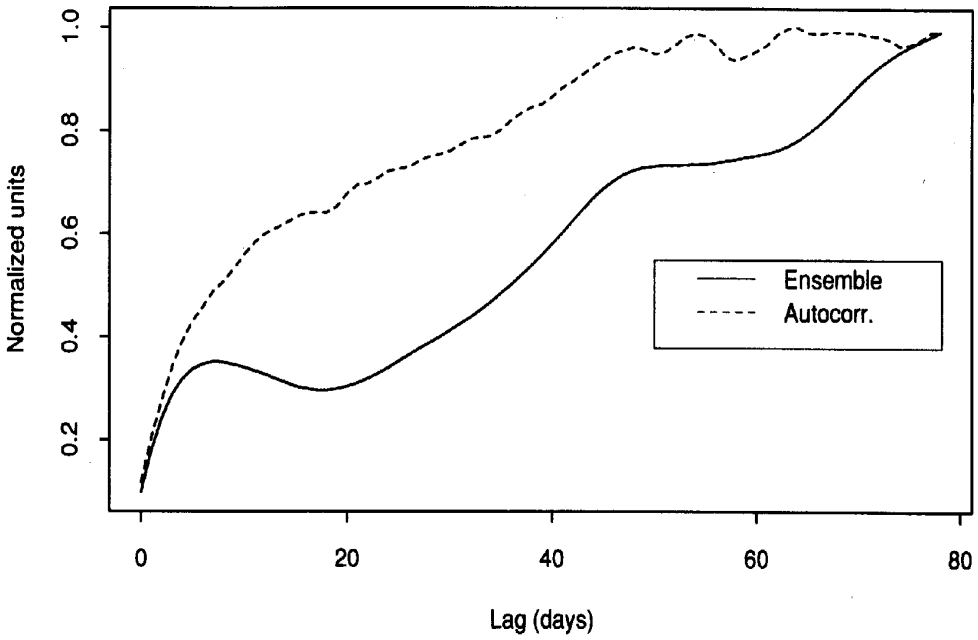

Fig. 27. Ensemble of the normalized response curve of simulations of the step function increase of the solar constan on a dry *Terra Blanda* (North et al., 1993).

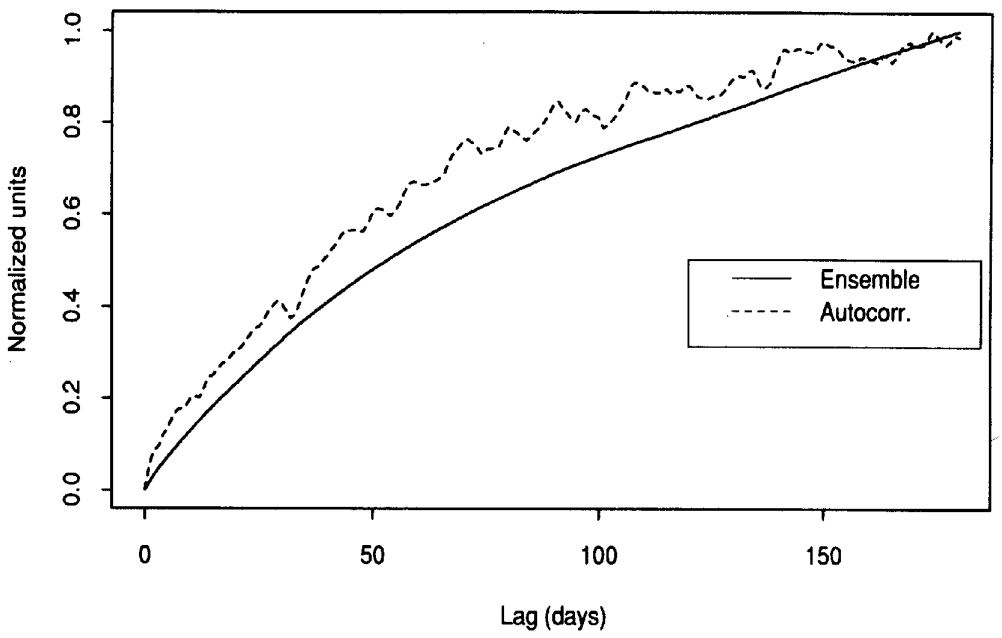

Fig. 28. Ensemble of the normalized response curve of simulations of the step function increase of the solar constant on a wet *Terra Blanda* (North et al., 1993).

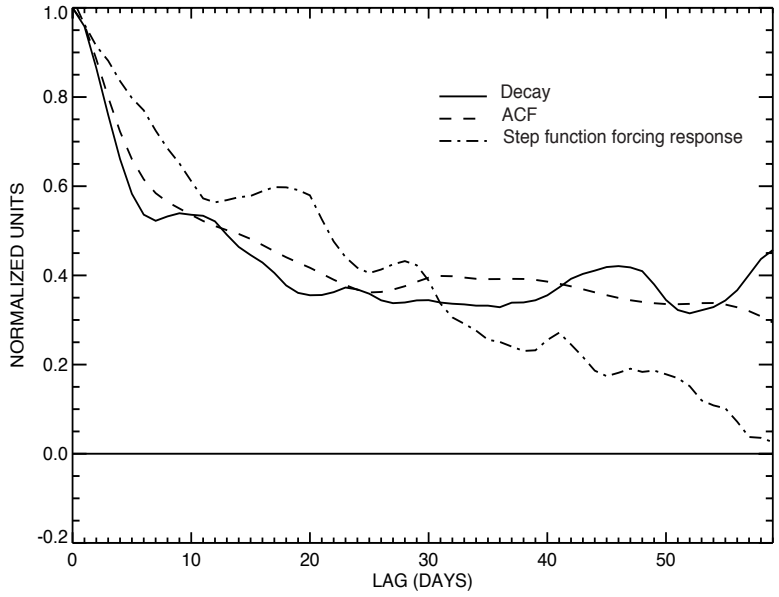

Fig. 29. Decay of the 2σ naturally occurring anomalies in T_{00}, the ensemble mean response of the global average temperature to the step solar forcing and the auto-correlation function of T_{00} on *Terra Blanda 3*

CHAPTER VI

RETURN PERIOD ANALYSIS

The probability distribution function of the spherical harmonic coefficients shows that they are approximately normally distributed over time. Figures 30, 31, and 32 show the probability distribution functions of T_{00}, T_{20}, and T_{40}. To analyze the extremes (tails) of these normal distributions, a different manner of plotting the tail is employed. The recurrence period of deviations from the means are plotted to give a more lucid picture of the extreme values of the spherical harmonic coefficients. If $F(x)$ is the cumulative probability distribution function of a distribution, then the return period of a value of x is given by:

$$R(x) = \frac{1}{1 - F(x)} \tag{6.1}$$

i.e on an avergae a value greater than x occurs once every $R(x)$ time interval.

Figure 33 and Fig. 34 show the return period plots of anomalies of T_{00} and T_{20}, and Figure 35 and Fig. 36 show the return period plots of anomalies T_{40} and T_{80}. The horizontal axis represents the anomalies in units of the standard deviation and the vertical axis represent the return period in number of days. The return period of a normal distribution is also shown with each of these plots. It is noted that the plots come closer to the normal distribution curve with increasing degree of the spherical harmonic coefficient. This is explained by the resemblance of the spherical harmonic coefficients to an AR1 process, as shorter auto-correlation times imply smaller sampling errors because there are more independent samples.

As the degree of the spherical harmonic increases, the auto-correlation time decreases, as is seen in Fig. 10, which implies that the value of λ in equation 4.12 comes closer to zero, making the distribution more like white noise, which is normally dis-

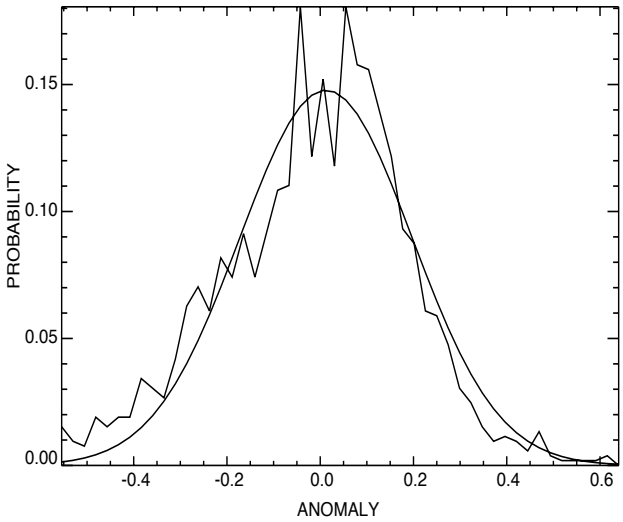

Fig. 30. Probability density function of T_{00} for *Terra Blanda 3*

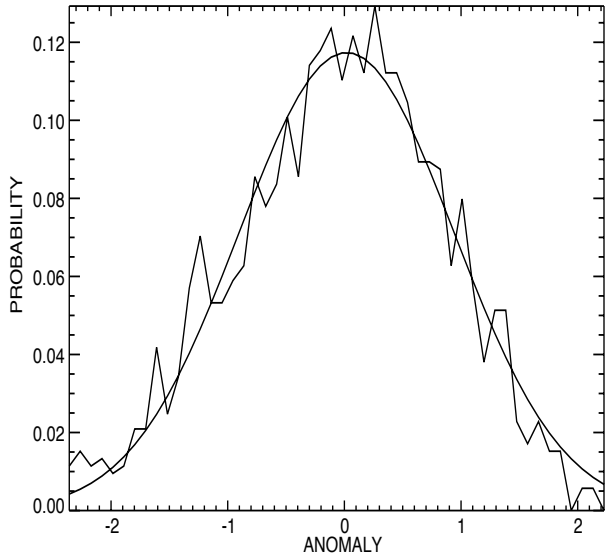

Fig. 31. Probability density function of T_{20} for *Terra Blanda 3*

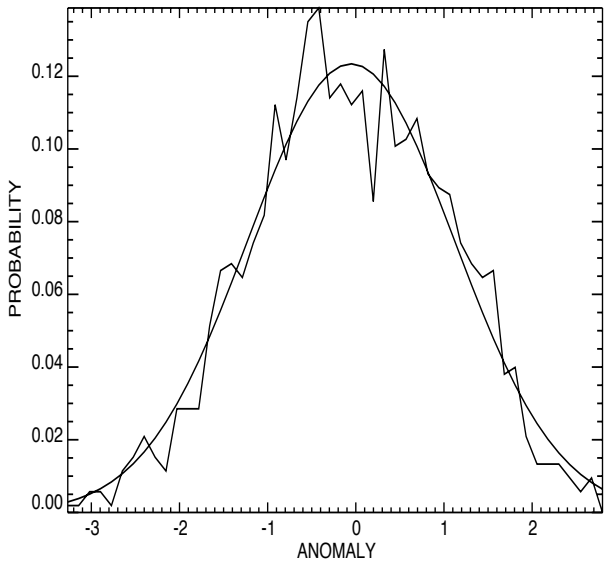

Fig. 32. Probability density function of T_{40} for *Terra Blanda 3*

tributed. Thus, the higher harmonics are more Gaussian than the lower ones, as is exhibited by the tail of the distribution functions. Also, because the spherical harmonic coefficients exhibit auto-correlation, the sample size is effectively reduced by a factor of the auto-correlation time. Since, the autocorrelation time of T_{00} is greater than that of higher harmonics, the sampling error of T_{00} is also greater than the higher harmonics. Modeling T_{00} by an AR1 process of autocorrelation time validates the above argument. An ensemble of 100 such AR1 processes is generated for a run of 1510 days, the same as that of T_{00}. The mean of the realizations is plotted along with the sampling interval of 95% confidence in Figure 37. Also shown is the Gaussian distribution return period curve and the return period curve of T_{00}. Both the Gaussian and the T_{00} curves lie within the sampling error of the AR1 simulation. As the run time of the AR1 realizations is increased the return period curve of the AR1 process comes close to the Gaussian curve. Figure 38 shows the return period curve of an ensemble of AR1 simulations for a run of about 800 auto-correlation times (20,000 days). The sampling error is reduced and the curve is closer to the Gaussian distribution curve.

To have a quantitative perspective on the sampling error, it is worthwhile to evaluate the length of data record required for predicting the return period of an anomaly with 95% confidence level small enough to lie within two auto-correlation times. Using the data from the ensemble of AR1 processes of the 1510 day run, it is evaluated that the data record required for predicting the return period of a 2σ anomaly within a 95% confidence level within 2 auto-correlation times is around 16 auto-correlation times (400 days), and for predicting the return period of a 2.5σ anomaly for the same confidence interval is around 1600 auto-correlation times (38,000 days). Thus, if an AR1 process is considered to be an apt representation of the spherical harmonic coefficients, and is used to model the global averaged temperature

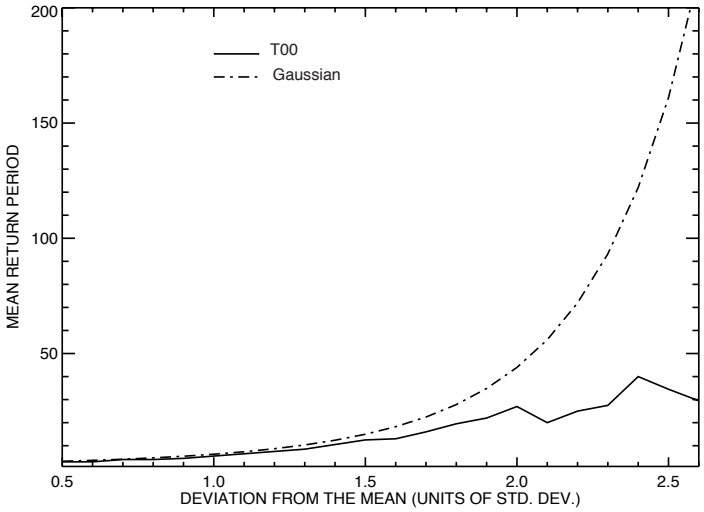

Fig. 33. Return period of T_{00} anomalies along with the ideal normal distribution.

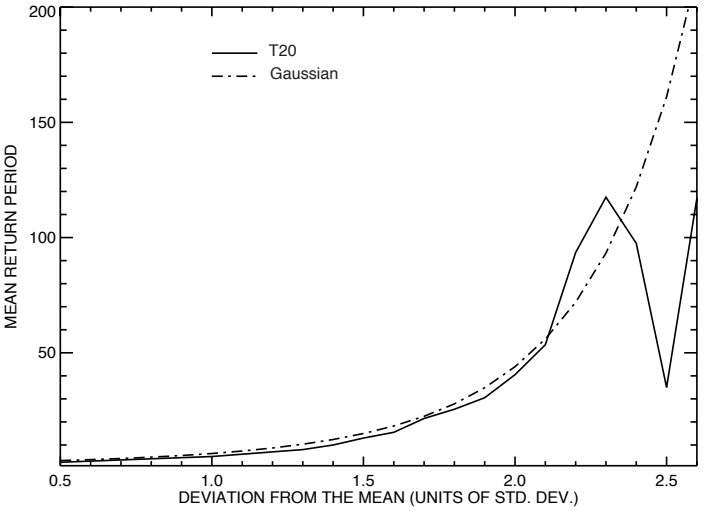

Fig. 34. Return period of T_{20} anomalies along with the ideal normal distribution.

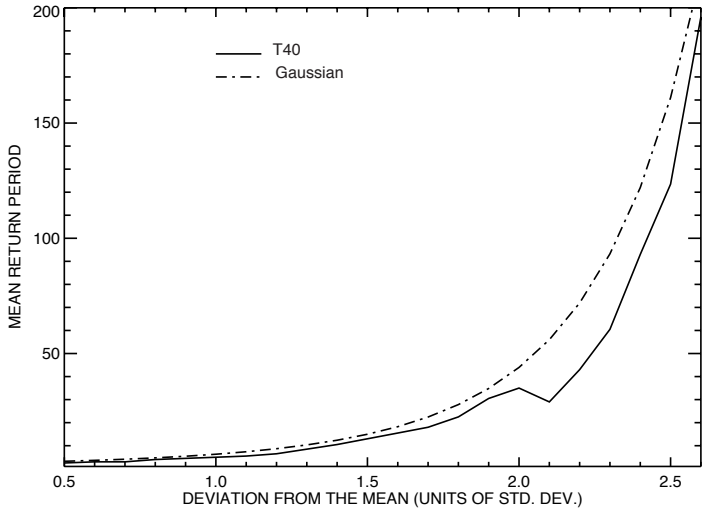

Fig. 35. Return period of T_{40} anomalies along with the ideal normal distribution.

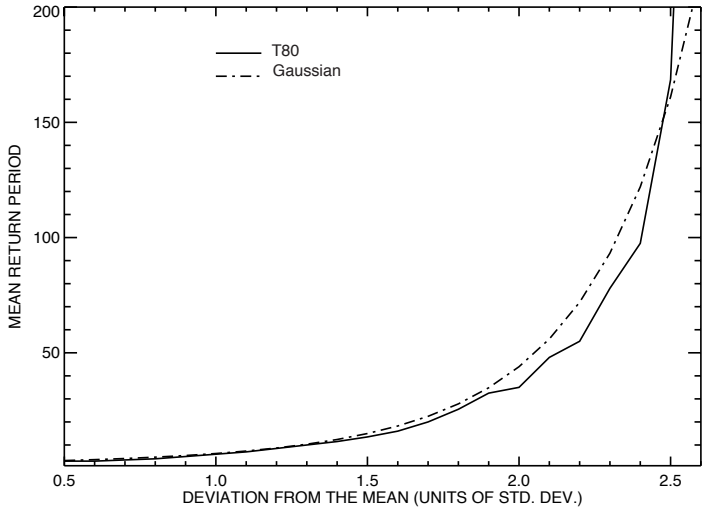

Fig. 36. Return period of T_{80} anomalies along with the ideal normal distribution.

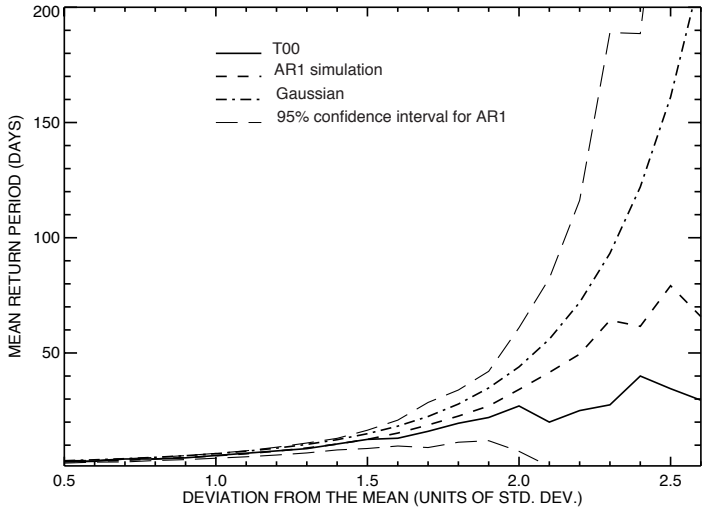

Fig. 37. Return period of an AR1 simulation of T_{00} run for 1510 days along with the 95% confidence interval.

of Terra Blanda 3, then the return period plot of an AR1 process of a significant data length can be used for analysis of the return period of extremes of global average temperature.

Another approach to analyzing the extreme values for fairly rare occurrences of the global average temperature is to study the return period of the maximum value of a block of days. The size of the block in this study is taken to be two auto-correlation times, so that each of the blocks become approximately statistically independent of each other. There would never be enough data to analyze rare events accurately, simply by definition. The AR1 model of T_{00} is used, since the data from Terra Blanda 3 is very short for the study of rare occurrences as has been demonstrated above by considering the tail of the normal distribution. The distribution of the maximum of a block of days is the Generalized Extreme Values distribution, $G(z)$. The AR1 model is run for various number of days to study the return period of the maximum of 50

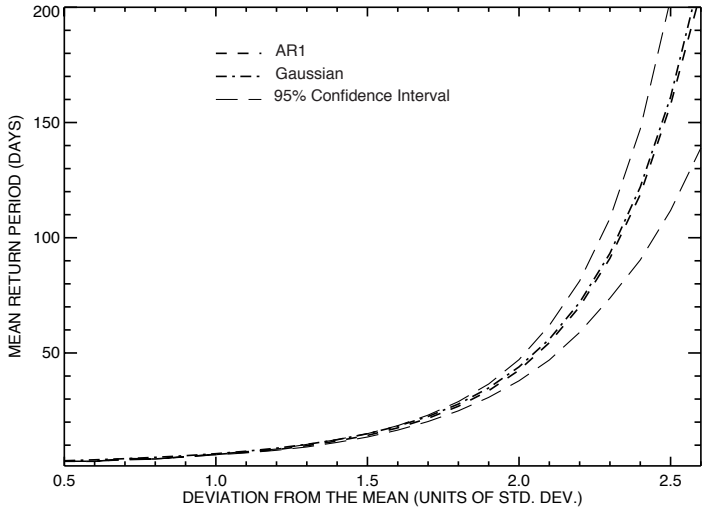

Fig. 38. Return period of an AR1 simulation of T_{00} run for 800 auto-correlation times (20,000 days) along with the 95% confidence interval.

days. Figure 39 shows the return period of anomalies obtained from the AR1 run of 21,000 auto-correlation times (500,000 days). Also, shown is the return period of the Gaussian and the GEV distribution fit with the location and shape parameters the same as the AR1 simulation. The shape factor was found to be 0.245. The generalized extreme value distribution fits modestly with the data obtained from the simulated AR1 process, verifying the extreme value theory.

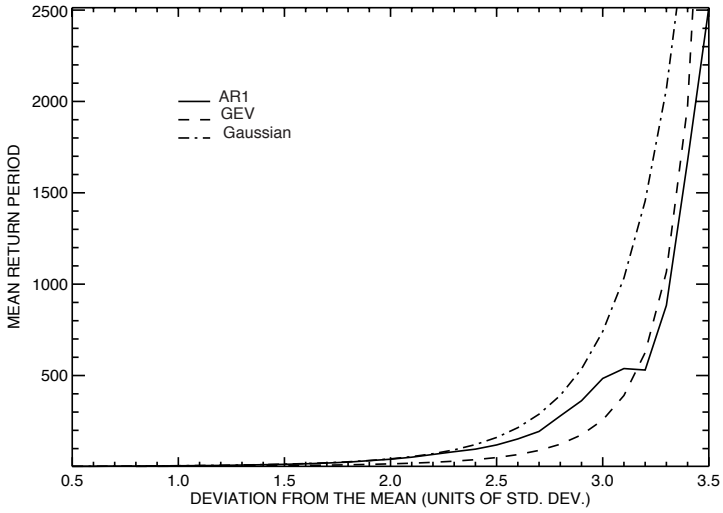

Fig. 39. Return period of block maxima of an AR1 simulation of T_{00} run for 21,000 auto-correlation times (500,000 days) along with the generalized extreme distrbution fit and Gaussian distribution.

CHAPTER VII

SUMMARY

CCM3 is run for 1510 days on Terra Blanda 3 and the surface temperature field thus obtained is decomposed into its spectral components to study the spatial and temporal spectra. Length scale of the simulation is found to be in agreement with the the real world data and also with CCM0. The auto-correlation time of the surface temperature field on Terra Blanda 3 is found to be 24 days for the spherical harmonic coefficient T_{00} and is found to be 10 and 8 days for the spherical harmonic coefficients T_{20} and T_{40} respectively.

The simulated model is then forced with a sinusoidal forcing of the sun with a period of 30 days and the response of T_{00}, T_{20} and T_{40} is observed to be quite linear. The model is also forced with a steady heat source 15 ° wide located at the mid-latitudes on both the hemispheres with heating densities of 5, 30 and 50 W/m^2. The response of the forcing at the center of the heat source is found to be fairly linear to the amplitude of the response. The above imply that the first moment response of the model is closely linear. The response of the surface temperature field to the 50 W/m^2 forcing is compared to that of a similar experiment using CCM0 and the EBM. It is found that CCM0 is closer to the EBM than CCM3, implying somewhat greater complexity in CCM3, and perhaps its closer resemblance to the real world.

Fluctuation dissipation is tested for applicability on CCM3. The ensemble response of a step function solar forcing is found to be closely related to the decay of naturally occurring anomalies and the auto correlation function. The above are related more closely in CCM3 than they did for CCM0. Since, we think CCM3 is closer to the real world more evidence is accumulated suggesting that the fluctuation dissispation theorem can be applied approximately to the real Earth system.

Return period analysis is attempted on the surface temperature data obtained from the run. It is observed that the 1510 day data is not sufficient for making such an analysis for large anomalies mainly due to the obvious fact that extreme events have rare occurrences, and are not observed in short runs. An AR1 simulation was used to demonstrate the sampling error associated with a length of data equal to the run of CCM3.

REFERENCES

Acker T. L., L. E. Buja, J. M. Rosinski, J. E. Truesdale, 1996: User's guide to NCAR CCM3, NCAR/TN-421+1A

Bell, T. L., 1985: Climatic sensitivity and fluctuation-dissipation relations. *Turbulence and Predictability in Geophysical Fluid Dynamics and Climate Dynamics*, 424–440.

Briegleb, B. P., 1992: Delta-Eddington approximation for solar radiation in the NCAR Community Climate Model. *J. Geophys. Res.*, **97**, 7603–7612.

Chervin, R. M., 1986: Interannual Variability and seasonal climate predictability. *J. Atmos. Sci.*, **43**, 233–251.

Coles, S., 2001: *An Introduction to statistical modeling of extreme values.* Springer, London.

Frei, C., 2003: Statistical Limitations for diagnosing changes in extremes from climate model simulations. *AMS Symp. Global Change Clim. Var.*, **14**.

Hansen, J., S. Lebedeff, 1987: Global trends of measured surface air temperature. *J. Geophys. Res.*, **92**, 13345–13372.

Hasselmann, K., 1979: On the signal-to-noise problem in atmospheric response studies. *Meteorology over the Tropical Oceans*, D. B. Shaw, Ed., Roy. Meteor. Sci., 251–259.

Huang J-P, K.-J. J. Yip, G. R. North, 1991: Circulation statistics for Terra Blanda, CSRP, Tech Rep No. 1.

Kharin V. V., F. W. Zwiers, 2000: Changes in the extremes in an ensemble of transient climate simulations with a coupled Atmosphere-Ocean GCM. *J. Climate*, **13**, 3760–3788.

Kiehl, J. T., J. J. Hack, G. B. Bonan, B. P. Briegleb, D. L. Williamson, P. L. Rasch, 1996: Description of the NCAR Community Climate Model (CCM3), NCAR/TN-420+STR.

Kiehl, J. T., J. J. Hack, B.P. Briegleb, 1994: The simulated earth radiation budget of the NCAR CCM2 and comparisons with the earth's radiation budget experiment (ERBE). *J. Geophys. Res.*, **99**, 20815–20827.

Leith, C. E., 1975: Climate response and fluctuation dissipation. *J. Atmos. Sci.*, **32**, 2022–2026.

Leung, L.-Y., G.R. North, 1991: Atmospheric variability on a zonally symmetric land planet. *J. Climate*, **4**, 753–765.

Lorenz, E. N., 1979: Forced and Free Variations in weather and climate. *J. Atmos. Sci.*, **36**, 1367–1376.

McGuffie K., A. Henderson-Sellers, 1997: *A Climate Modelling Primer.* John Wiley and sons, New York.

North, G. R, 1984: The small ice-cap instability in diffusive climate models. *J. Atmos. Sci.*, **41**, 3390–3395.

North, G. R, R. F. Cahalan, 1981: Predictability in a solvable stochastic climate model. *J. Atmos. Sci.*, **38**, 504–513.

North, G. R, K.-J.J. Yip and L.-Y. Leung, 1992: Forced and free variations of the surface temperature field in a general circulation model. *J. Climate*, **5**, 227–239.

North, G. R., R. E. Bell and J. W. Hardin, 1993: Fluctuation dissipation in a general circulation model. *Climate Dyn.*, **8**, 259–264.

Stone, P., 1978: Baroclinic Adjustment. *J. Atmos. Sci.*, **35**, 561–571.

Williamson, D.L., P. J. Rasch, 1994: Water vapor transport in the NCAR CCM2. *Tellus*, **42A**, 34–51.

Zhang, X., F. W. Zweirs, G. Li, 2004: Monte Carlo Experiments on the detection of trends in Extreme Values. *J. Climate*, **17**, 1945–1952.

VITA

Salil Mahajan received a Bachelor's Degree in architecture from the Indian Institute of Technology, Kharagpur, India in 2002. He then came to the Texas A&M University to pursue a Master's Degree in urban planning, but developed interest in atmospheric sciences and was admitted to the Department of Atmospheric Sciences at Texas A&M University in September 2003 to pursue a Master's degree. He can be reached at the Department of Atmospheric Sciences, Texas A&M University, College Station, 77843-3150. Email: salilmahajan@neo.tamu.edu.

The typist for this thesis was Salil Mahajan.